Journal of Physiology (1990), **425**, *pp.* 85–115
With 15 *figures*
Printed in Great Britain

REGULATION OF THE INTRACELLULAR FREE CALCIUM CONCENTRATION IN SINGLE RAT DORSAL ROOT GANGLION NEURONES *IN VITRO*

BY STANLEY A. THAYER* AND RICHARD J. MILLER

From the Department of Pharmacological and Physiological Sciences, University of Chicago, 947 East 58th Street, Chicago, IL 60637, USA

(*Received 31 May 1989*)

SUMMARY

1. Simultaneous whole-cell patch-clamp and Fura-2 microfluorimetric recordings of calcium currents (I_{Ca}) and the intracellular free Ca^{2+} concentration ($[Ca^{2+}]_i$) were made from neurones grown in primary culture from the dorsal root ganglion of the rat.

2. Cells held at −80 mV and depolarized to 0 mV elicited a I_{Ca} that resulted in an $[Ca^{2+}]_i$ transient which was not significantly buffered during the voltage step and lasted long after the cell had repolarized and the current ceased. The process by which the cell buffered $[Ca^{2+}]_i$ back to basal levels could best be described with a single-exponential equation.

3. The membrane potential *versus* I_{Ca} and $[Ca^{2+}]_i$ relationship revealed that the peak of the $[Ca^{2+}]_i$ transient evoked at a given test potential closely paralleled the magnitude of the I_{Ca} suggesting that neither voltage-dependent nor Ca^{2+}-induced Ca^{2+} release from intracellular stores made a significant contribution to the $[Ca^{2+}]_i$ transient.

4. When the cell was challenged with Ca^{2+} loads of different magnitude by varying the duration or potential of the test pulse, $[Ca^{2+}]_i$ buffering was more effective for larger Ca^{2+} loads. The relationship between the integrated I_{Ca} and the peak of the $[Ca^{2+}]_i$ transient reached an asymptote at large Ca^{2+} loads indicating that Ca^{2+}-dependent processes became more efficient or that low-affinity processes had been recruited.

5. Inhibition of Ca^{2+} influx with neuropeptide Y demonstrated that inhibition of a large I_{Ca} produced minor alterations in the peak of the $[Ca^{2+}]_i$ transient, while inhibition of smaller currents produced corresponding decreases in the $[Ca^{2+}]_i$ transient. Thus, inhibition of the I_{Ca} was reflected by a change in the peak $[Ca^{2+}]_i$ only when submaximal Ca^{2+} loads were applied to the cell, implying that modulation of $[Ca^{2+}]_i$ is dependent on the activation state of the cells.

6. Intracellular dialysis with the mitochondrial Ca^{2+} uptake blocker Ruthenium Red in whole-cell patch-clamp experiments removed the buffering component which

* Present address to which correspondence should be sent: Department of Pharmacology, University of Minnesota Medical School, 435 Delaware Street S.E., Minneapolis, MN 55455, USA.

MS 7718

was responsible for the more efficient removal of $[Ca^{2+}]_i$ observed when large Ca^{2+} loads were applied to the cell.

7. When cells were superfused with 50 mM-K^+, $[Ca^{2+}]_i$ transients recorded from the cell soma returned to control levels very slowly. Pharmacological studies indicated that mitochondria were cycling Ca^{2+} during this sustained elevation in $[Ca^{2+}]_i$. In contrast, $[Ca^{2+}]_i$ transients recorded from cell processes returned to basal levels relatively rapidly.

8. Extracellular Na^+-dependent Ca^{2+} efflux did not significantly contribute to buffering $[Ca^{2+}]_i$ transients in dorsal root ganglion neurone cell bodies. Furthermore, calmodulin antagonists and sodium orthovanadate applied via the patch pipette were without effect on Ca^{2+} buffering. Thus, the Na^+–Ca^{2+} exchange system does not participate in Ca^{2+} buffering in the cell bodies of dorsal root ganglion neurones and the ATP-dependent processes which presumably participate in removing Ca^{2+} from the cytosol do not seem to be regulated in the same manner as the Ca^{2+}–Mg^{2+}-ATPase previously characterized from erythrocytes.

INTRODUCTION

Calcium regulates neuronal excitability as well as participating in the release of neurotransmitters. Thus modulation of $[Ca^{2+}]_i$ is an important means of regulating diverse neuronal functions. $[Ca^{2+}]_i$ can be potentially elevated by mobilization from intracellular stores (Kuba, 1980; Streb, Irvine, Berridge & Schulz, 1983), by influx via voltage-sensitive (Tsien, 1983) and receptor-operated (Mayer & Westbrook, 1987) Ca^{2+} channels or by reversal of the electrogenic Na_o^+–Ca_i^{2+} exchanger (Barcenas-Ruiz, Beuckelmann & Wier, 1987). However, the mechanisms by which $[Ca^{2+}]_i$ signals are buffered back to basal levels (approximately 10^{-7} M) are not well characterized in neurones. Data from a variety of tissues have suggested that four processes may be important: $[Ca^{2+}]_i$ transients could be potentially buffered by (i) binding to cytosolic proteins, (ii) uptake into mitochondria, (iii) ATP-dependent sequestration or efflux and (iv) extracellular Na^+-dependent efflux (reviewed by Carafoli, 1987).

Calcium homeostasis has been studied in a wide range of neuronal preparations including squid giant axons (Baker & Dipolo, 1984), slices of mammalian brain (Tank, Sugimori, Connor & Llinas, 1988), optic nerve (Lev-Ram & Grinvald, 1987) and synaptosomes (Blaustein, 1988). $[Ca^{2+}]_i$ transients evoked by depolarizing stimuli have been recorded in mammalian sensory (McBurney & Neering, 1985) and spinal cord neurones (Mayer, MacDermott, Westbrook, Smith & Barker, 1987) as well as the cell bodies (Gorman & Thomas, 1980; Boyle, Klein, Smith & Kandel, 1984) and terminals (Connor, Kretz & Shapiro, 1986; Ross, Arechiga & Nicholls, 1987; Ross & Graubard, 1989) of invertebrate neurones. Although $[Ca^{2+}]_i$ buffering rates have varied in these different studies, the $[Ca^{2+}]_i$ transients observed have consistently proved to last long after repolarization of the cell. Thus it appears that $[Ca^{2+}]_i$ signals may be able to modulate Ca^{2+}-dependent processes in the cell long after the stimulus which gave rise to them has ceased. In spite of the slow kinetics of this process neurones do possess very effective mechanisms for buffering Ca^{2+}. These have been estimated to leave less than 1 % of the Ca^{2+} entering the cell free in

the cytosol at the peak of the transient (McBurney & Neering, 1985). Furthermore, the Ca^{2+} buffering capacity of neurones has been shown to increase with increasing Ca^{2+} loads (Ahmed & Connor, 1988). In general, however, the relationship between Ca^{2+} loads and the processes which buffer them thereby producing transient $[Ca^{2+}]_i$ signals is not clear. This is particularly true in vertebrate neurones which are difficult to study because of their small size.

We have previously described methods for monitoring rapid $[Ca^{2+}]_i$ signals in vertebrate neurones while making simultaneous electrophysiological recordings (Thayer, Sturek & Miller, 1988*c*). In the present series of experiments we used this technique to analyse those processes that are important in regulating changes in $[Ca^{2+}]_i$ following challenge of rat DRG neurones *in vitro* with quantifiable Ca^{2+} loads.

A preliminary report of this work has appeared (Thayer & Miller, 1988).

METHODS

Instrumentation. The instrumentation used in these experiments has been described in detail elsewhere (Thayer *et al.* 1988*c*). For excitation of the Fura-2, a collimated light beam from a 200 W mercury arc lamp was passed through a dual-beam spectrophotometer (Phoenix Instruments) which alternated wavelengths from 340 to 380 nm by means of a chopper spinning at a frequency of 60 Hz. The light source was placed on a table outside of a light-tight Faraday cage which enclosed the vibration isolation table supporting the microscope. In place of the original sample chamber, a fused silica lens was positioned to focus the light onto the end of a liquid light guide (3 mm × 1 m, Oriel, Stratford, CT, USA). On the other end of the liquid light guide a similar lens was positioned for directing light through the epi-fluorescence illuminator of the inverted microscope (Diaphot, Nikon). The light was reflected off a dichroic mirror (Nikon, DM 400) and focused through a × 70 phase-contrast oil-immersion objective (E. Leitz Inc., Rockleigh, NJ, USA; numerical aperture 1·15). The emission fluorescence was selected for wavelength with a 480 nm barrier filter and recordings were defined spatially with a rectangular diaphragm. The diaphragm was mounted on the video port such that it could be rotated, thus allowing the definition of rectangular areas at off-axis angles. This flexibility was useful for circumscribing a neuronal process extending from a cell at an angle, for example. The fluorescence emission was analysed with a photomultiplier tube (bialkali) and discriminator (APED II; Thorn EMI Gencom Inc., Plainview, NY, USA). The discriminator output was converted to pulses which were then integrated by passing the signal through an 8-pole low-pass Bessel filter at 500 Hz. The gain on this detection system could be adjusted from 1 to 100 × by increasing the length of these pulses. The conversion of light intensity to voltage by this process was confirmed to be linear over the range of light levels used in these experiments. The signal from the filter was fed into one channel of an analog-to-digital converter PDP-11/73 computer system (Indec Systems, Sunnyvale, CA, USA). The signals from two photodiodes, each placed in a small portion of the light beam directed towards the monochromators, were fed into two additional channels of the analog-to-digital converter.

Sorting the fluorescence output into signals corresponding to excitation at each of the two wavelengths was performed entirely with software. All software was written in BASIC-23 (Cheshire Data, Indec Systems). The photomultiplier output was sorted into signals from 340 and 380 nm excitation by using the photodiode outputs as timing signals.

Perfusion chamber. The recording chamber consisted of a Plexiglas block machined to accommodate a 25 mm round cover-glass as a bottom. The cover-glass was held in place by a steel ring secured by four nuts threaded onto studs which protrude from the Plexiglas. The underside of the chamber was machined flat so that pressure from the ring would hold the cover-glass tightly onto the Plexiglas without cracking or leaking. The 41 mm ring diameter fitted precisely within the opening of the microscope stage (Diaphot, Nikon, Garden City, NY, USA) such that the perfusion chamber was seated squarely on the stage with the ring protruding below. Three reservoirs were cut into the block such that a thin sheet of buffer flowed out of the inlet reservoir, across the cells in the experimental chamber, and was drawn up across nylon mesh to the efflux reservoir for

evacuation by suction. The solution exchange in the cell superfusion system approximated a step occurring over 10 s. The tubing between the large media reservoirs and the inlet to the chamber delayed the onset of the solution exchange by an additional 10 s. This perfusion chamber was mounted on an inverted microscope and cells or portion of cells were localized by standard phase-contrast illumination.

Calibration and analysis. Records were corrected for experimentally determined background values and the ratios re-calculated off-line. Ratios were converted to free $[Ca^{2+}]$ by using the equation $[Ca^{2+}] = K(R-R_{min})/(R_{max}-R)$ in which R is the 340/380 nm fluorescence ratio (Grynkiewicz, Poenie & Tsien, 1985). The maximum ratio (R_{max}), the minimum ratio (R_{min}) and the constant K (K is the product of the dissociation constant for Fura-2 and the ratio of the free and bound forms of the dye at 380 nm) were determined from a curve fitted to a standard curve using the above equation with a non-linear least-squares fit computer program. The standard curve was determined for the Fura-2 pentapotassium salt in calibration buffer (which contained, in mM: 4-(2-hydroxethyl)-1-piperazineethanesulphonic acid (HEPES), 20; KCl, 120; NaCl, 5; $MgCl_2$,1; pH 7·1) containing 10 mM-ethyleneglycol-bis(β-aminoethylether)-*N,N,N',N'*-tetraacetic acid (EGTA), $K_s = 3{\cdot}969 \times 10^6$ M^{-1} (Fabiato & Fabiato, 1979), with calculated amounts of Ca^{2+} added to give free Ca^{2+} concentrations ranging from approximately 0 to 2000 nM. Experiments run over long periods of time (> 30 s) were digitally filtered with an algorithm which added one-half of the value of each data point to one-quarter of the value of each of the two neighbouring points. The data were cycled through this routine five times (cut-off frequency approximately 0·5 Hz). $[Ca^{2+}]_i$ traces in patch-clamp experiments were digitally filtered by a single cycle through an eleven-point moving-average algorithm (cut-off frequency approximately 8 Hz).

Cell culture. Neurones were cultured from the dorsal root ganglia (DRG) of neonatal rats essentially as described by Thayer, Perney & Miller (1988*b*). Briefly, 1- to 3-day-old Sprague–Dawley rats were killed by decapitation with sharp scissors. Dorsal root ganglion (DRG) neurones were then dissected from thoracic and lumbar segments, incubated for 15 min at 37 °C in collagenase–dispase (0·8 and 6·4 units/ml), and dissociated into single cells by trituration through a Pasteur pipette. The cells were then plated on laminin–fibronectin-coated cover-glasses (No. 1, 25 mm diameter). Cells were fed every 2–3 days with Ham's nutrient mixture F-12 supplemented with 5% heat-inactivated rat serum, 4% 17-day embryonic extract, 50 ng/ml nerve growth factor, 4·4 mM-glucose, 2 mM-L-glutamine, 1% MEM, 100 × vitamins and penicillin–streptomycin (100 units/ml and 100 μg/ml, respectively). Cultures were maintained at 37 °C in a water-saturated atmosphere with 5% carbon dioxide.

Superfusion experiments. For experiments on intact cells, neurones were loaded with the dye by incubation in 2 μM-Fura-2 acetoxymethyl ester (Molecular Probes Inc., Eugene, OR, USA), which is membrane permeant, for 1 h at 37 °C in HEPES-buffered Hank's balanced salt solution (pH 7·45) containing 0·5% bovine serum albumin. The HEPES–Hank's solution was composed of (in mM): HEPES, 20; NaCl, 137; $CaCl_2$, 1·3; $MgSO_4$, 0·4; $MgCl_2$, 0·5; KCl, 5·0; KH_2PO_4, 0·4; $NaHPO_4$, 0·6; $NaHCO_3$, 3·0; and glucose, 5·6. Following the loading incubation, during which time the dye ester is hydrolysed by cytosolic esterases to the membrane-impermeant polycarboxylate anion that is Fura-2, the cells were washed twice in the HEPES–Hank's solution and incubated for 30 min. The cover-glasses containing the loaded and washed cells were then mounted in the perfusion chamber for viewing. Prior to initiating the recording each cell was routinely examined for the heterogeneous fluorescence that would indicate concentration of the dye in organelles (Malgaroli, Milani, Meldolesi & Pozzan, 1987). No such punctate fluorescence was observed. Depolarization-induced Ca^{2+} influx was produced by changing the perfusing solution from low K^+ (5 mM) to high K^+ (50 mM) with K^+ exchanged for Na^+ reciprocally. For experiments run over long periods of time (> 30 s), thirty ratios were determined in 1·1 s, the average ratio was displayed on-line, and the average intensity values for each wavelength were stored. After completion of a given experiment the microscope stage was adjusted so that no cells or debris occupied the field of view defined by the diaphragm and background light levels were determined.

Whole-cell patch clamp. The tight-seal whole-cell configuration of the patch-clamp technique (Hamill, Marty, Neher, Sakmann & Sigworth, 1981) was used to record transmembrane I_{Ca} from single cells while simultaneously measuring $[Ca^{2+}]_i$ transients. Cells were mounted in the perfusion chamber and thoroughly rinsed with a buffer composed of (in mM): tetraethylammonium chloride (TEA-Cl), 143; $CaCl_2$, 2; $MgCl_2$, 1; HEPES, 10; glucose, 10; pH adjusted to 7·4 with TEA-OH. A cell was then approached with a fire-polished pipette containing a solution composed of (in mM): Fura-2 pentapotassium salt, 0·1; CsCl, 135; $MgCl_2$, 1; HEPES, 10; ditris-phosphocreatine, 14;

MgATP, 3·6; 50 U/ml creatinine phosphokinase; pH adjusted to 7·1 with CsOH. The solutions described were chosen to isolate currents through Ca^{2+} channels from other currents (namely, sodium and potassium currents). Current-clamp experiments were performed with a pipette solution composed of (in mM): Fura-2 pentapotassium salt, 0·1; KCl, 135; $MgCl_2$, 1; HEPES, 10; ditris-phosphocreatine, 14; MgATP, 3·6; 50 U/ml creatinine phosphokinase; pH adjusted to 7·1 with KOH. Currents were recorded by a Yale Mark V amplifier with a 1·0 GΩ feedback resistor, filtered by an 8-pole low-pass Bessel filter with a cut-off frequency of 200 Hz and stored on the computer used for fluorescence data acquisition. Background fluorescence was recorded and pipette capacitance was zeroed after a gigaseal was formed, but before breaking into the cell. Thus, we could account for the fluorescence contributed by the Fura-2 in the pipette. Since the pipette approached the cell from above, the objective was focused below the pipette nearer the middle of the cell to minimize the detection of pipette fluorescence. Full diffusion of Fura-2 into the cell occurred over a period of 1–2 min. Cell capacitance was determined by integrating the unfiltered capacity transient resulting from a small voltage step and dividing by the amplitude of the step. The capacity transient was fitted to a decaying exponential and the *R–C* time constant was used to estimate series resistance. Series resistance values ranged from 2 to 7 MΩ and were partially compensated by the patch-clamp circuitry. Linear leak corrections were performed by first averaging sixteen 10 mV hyperpolarizing pulses from the holding potential. The DC component of the averaged leak current was then modelled so as to increase the signal-to-noise ratio. Digital summation of this leak template after appropriate scaling with the current obtained during depolarizing test pulses provided the leak correction. Cells were discarded when the steady leakage current at the holding potential was greater than 5% of the peak inward current. In some traces capacity transients were removed for clarity. All experiments were performed at room temperature.

RESULTS

Activation of I_{Ca} to apply Ca^{2+} loads to DRG neurones

Membrane depolarization activates three types of Ca^{2+} channels in chick and mouse DRG neurones (Nowycky, Fox & Tsien, 1985; Fox, Nowycky & Tsien, 1987; Kostyuk, Shuba & Savchenko, 1988). Figure 1 illustrates the I_{Ca} recorded in rat DRG neurones using the whole-cell configuration of the patch-clamp technique (Hamill *et al.* 1981); currents other than those carried by Ca^{2+} were blocked by ionic substitution. The currents were of similar magnitude and had similar voltage characteristics to those recorded from chick and mouse neurones suggesting that all three Ca^{2+} channel types may also be present in rat DRG cells. The $[Ca^{2+}]_i$ was also recorded in this experiment using microfluorimetric measurement of Fura-2 free acid introduced into the cell by dialysis with the solution contained in the patch pipette. The $[Ca^{2+}]_i$ was determined at a frequency of 60 Hz from the ratio of the fluorescence intensity measured when excited at 340 or 380 nm as described previously (Thayer *et al.* 1988*c* and in Methods). For the cell illustrated the current evoked by stepping to 0 mV from a holding potential of −80 mV peaked at close to 2 nA and resulted in an $[Ca^{2+}]_i$ transient that climbed from a basal level of 105 nM to peak at 438 nM. The average basal $[Ca^{2+}]_i$ in the whole-cell clamp was measured at the beginning of each experiment (after several moderate depolarizing stimuli but prior to treating the cell with any pharmacological agents) and found to be 136 ± 15 nM ($n = 40$). The peak of the $[Ca^{2+}]_i$ transient varied considerably (630 ± 55 nM for a 320 ms test pulse), depending on the magnitude of the I_{Ca} relative to the size of the cell. When the cell was held at a membrane potential of −50 mV the inward current evoked by stepping to 0 mV was greatly reduced and the resulting $[Ca^{2+}]_i$ transient was smaller as well (Fig. 1).

In the experiment described in Fig. 1 the $[Ca^{2+}]_i$ closely paralleled the influx of

Ca^{2+} via voltage-activated Ca^{2+} channels. In Fig. 2*A* the $[Ca^{2+}]_i$ and the integral of the I_{Ca} were scaled to illustrate the fact that the increase in $[Ca^{2+}]_i$ was directly proportional to the inward movement of charge across the membrane. This implies that the $[Ca^{2+}]_i$ transient was not significantly amplified by Ca^{2+}-induced Ca^{2+} release from intracellular stores of Ca^{2+} as found in the heart (Fabiato, 1985*a*, *b*; Callewaert,

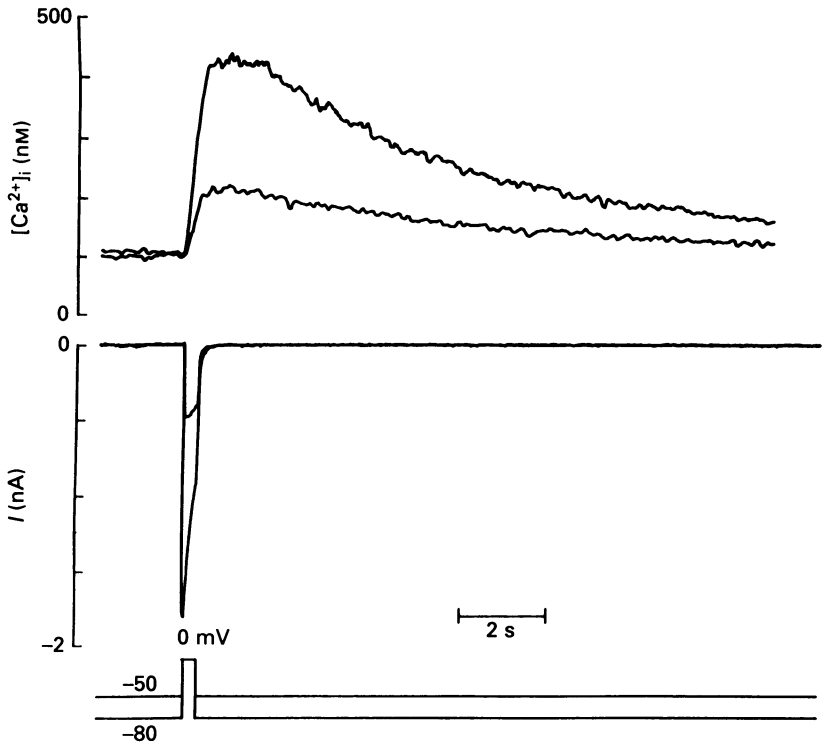

Fig. 1. $[Ca^{2+}]_i$ and I_{Ca} recordings from a DRG neurone held at either −80 or −50 mV and depolarized to 0 mV. The cell was voltage clamped using the whole-cell configuration of the patch-clamp technique and $[Ca^{2+}]_i$ was measured by introducing 100 μM-Fura-2 into the cell via the pipette solution. The smaller I_{Ca} and $[Ca^{2+}]_i$ transient correspond to the −50 mV holding potential.

Cleemann & Morad, 1988) or in sympathetic neurones (Lipscombe, Madison, Poenie, Reuter, Tsien & Tsien, 1988; Thayer, Hirning & Miller, 1988 *a*). We have previously shown that DRG neurones do possess caffeine- and ryanodine-sensitive intracellular Ca^{2+} stores, but these are small (Thayer *et al.* 1988*b*). Thus in these cells, as opposed to heart for example, the caffeine-sensitive intracellular Ca^{2+} store does not seem to appreciably amplify the magnitude of the $[Ca^{2+}]_i$ signal elicited by the influx of Ca^{2+} via voltage-sensitive Ca^{2+} channels in response to membrane depolarization. Furthermore as shown in Fig. 2, the proportionality remains constant over the course of the 320 ms voltage step suggesting that the rate of Ca^{2+} buffering in the cell was too slow to significantly alter $[Ca^{2+}]_i$ during the test pulse. For larger Ca^{2+} loads this was not necessarily the case as will be discussed in detail in a later section of this report.

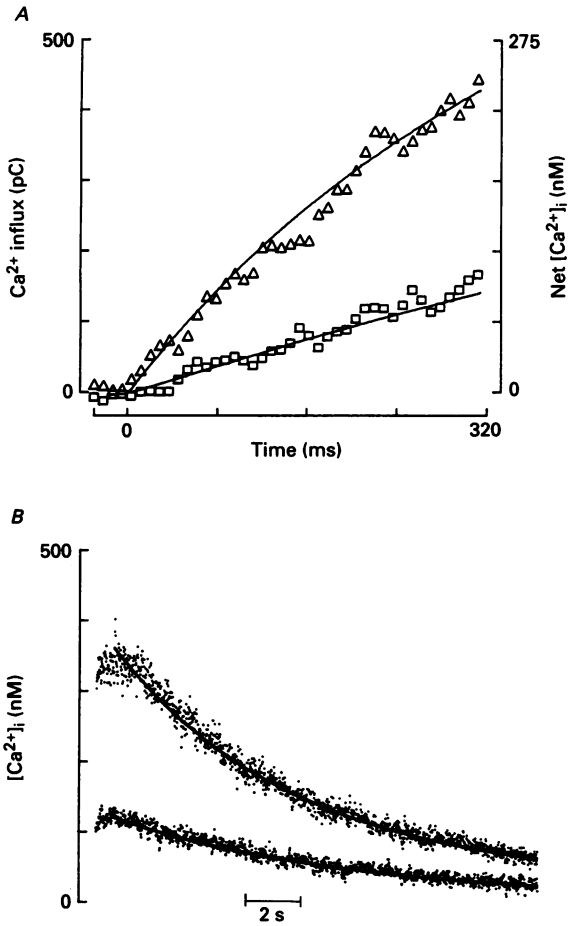

Fig. 2. The increase in $[Ca^{2+}]_i$ in response to a step depolarization is proportional to the I_{Ca} and the recovery is described by a single exponential. *A*, the traces displayed in Fig. 1 were expanded during the 320 ms test pulse to 0 mV. The inward currents were integrated and are displayed as continuous lines. The $[Ca^{2+}]_i$ determined from a 340/380 nm fluorescence ratio calculated approximately every 8 ms is plotted as open symbols (−80 mV hold, △; −50 mV hold, □). *B*, the recovery of the $[Ca^{2+}]_i$ transients (points) is described by single exponentials (continuous lines) with time constants of 5·4 and 6·7 s for the −80 and −50 mV holding potentials respectively. Curves were fitted by a non-linear least-squares fit computer program. Data displayed in this figure were not digitally filtered.

The small effect of Ca^{2+} buffering on the $[Ca^{2+}]_i$ transient over the course of the test pulse in this experiment is consistent with the slow rate of Ca^{2+} buffering seen after repolarization (Fig. 1). The slow Ca^{2+} buffering rate seen in this experiment is similar to the rates reported for mammalian central neurones (Mayer *et al.* 1987) and invertebrate neurones (Gorman & Thomas, 1980; Ross *et al.* 1987; Ahmed & Connor, 1988). The Ca^{2+} buffering process can be described by a single-exponential equation

(Fig. 2*B*) in agreement with the results of similar experiments performed in molluscan sensory neurones (Ahmed & Connor, 1988) but in contrast to the results found in rat spinal cord neurones (Mayer *et al.* 1987). Time constants were determined by a non-linear least-squares computer curve-fitting routine and found to be 5·4 and 6·7 s for the large (−80 mV hold) and small (−50 mV hold) transient, respectively. This difference does not appear to be due to a voltage dependence of recovery as indicated by experiments in which the pre- and test pulse potentials were held constant (at −80 and 0 mV, respectively) and the potential during recovery was varied between −40 and −100 mV without a detectable effect on the rate of recovery.

The membrane voltage versus I_{Ca} and $[Ca^{2+}]_i$ transient relationship

The current–voltage relationship for rat DRG neurones was similar to that found in DRG neurones from the chick (Fox *et al.* 1987; Fig. 3), which have been shown to possess three types of Ca^{2+} channels. For rat DRG neurones stepping to more positive test potentials from a holding potential of −100 mV elicited the small T-type current at test pulses positive to −70 mV. A representative sweep stepping to −40 mV shows this low-threshold activated current and the small $[Ca^{2+}]_i$ transient that resulted (Fig. 3*B*). Stepping to −20 mV, which elicited the peak I_{Ca} and presumably activated both the transient N-type and more sustained L-type Ca^{2+} channels, produced a much larger $[Ca^{2+}]_i$ transient as well (Fig. 3*C*). In comparison to previous reports using chick DRG neurones the peak current was shifted in the hyperpolarizing direction presumably because of elevated $[Ca^{2+}]_i$. Usually $[Ca^{2+}]_i$ is suppressed with chelators but they are not compatible with the Fura-2 measurements described here. The peak of the $[Ca^{2+}]_i$ transient closely paralleled the magnitude of the I_{Ca} again suggesting that neither voltage-dependent nor Ca^{2+}-induced release of Ca^{2+} from intracellular stores made a significant contribution to the $[Ca^{2+}]_i$ transient.

$[Ca^{2+}]_i$ buffering measured at varying Ca^{2+} loads

To determine the Ca^{2+} buffering characteristics of DRG neurones under various Ca^{2+} loading conditions cells were held at −80 mV in the whole-cell patch-clamp configuration and depolarized for different test pulse durations or to different test potentials in order to apply Ca^{2+} loads of different magnitudes. Figure 4 illustrates an experiment in which a neurone was depolarized from a holding potential of −80 mV to a test potential of 0 mV for test pulse durations ranging from 10 to 2560 ms. As expected, longer test pulses passed more current across the plasma membrane, resulting in larger $[Ca^{2+}]_i$ transients. Interestingly, at longer test pulse durations the increase in $[Ca^{2+}]_i$ was no longer proportional to the amount of Ca^{2+} that passed into the cell (Fig. 5). Note that increasing Ca^{2+} influx by elevating extracellular Ca^{2+} to 10 mM shifted the asymptote of the test pulse duration *versus* $[Ca^{2+}]_i$ curve to shorter test pulse durations while the decreased Ca^{2+} influx measured in 1 mM-extracellular Ca^{2+} following time-dependent Ca^{2+} channel inactivation shifted the asymptote to longer test pulses.

A decrease in current was observed during the test pulse presumably resulting from a combination of voltage- and Ca^{2+}-dependent inactivation. Thus, some degree of non-linearity might be expected in these curves when the decay of the I_{Ca} seen over

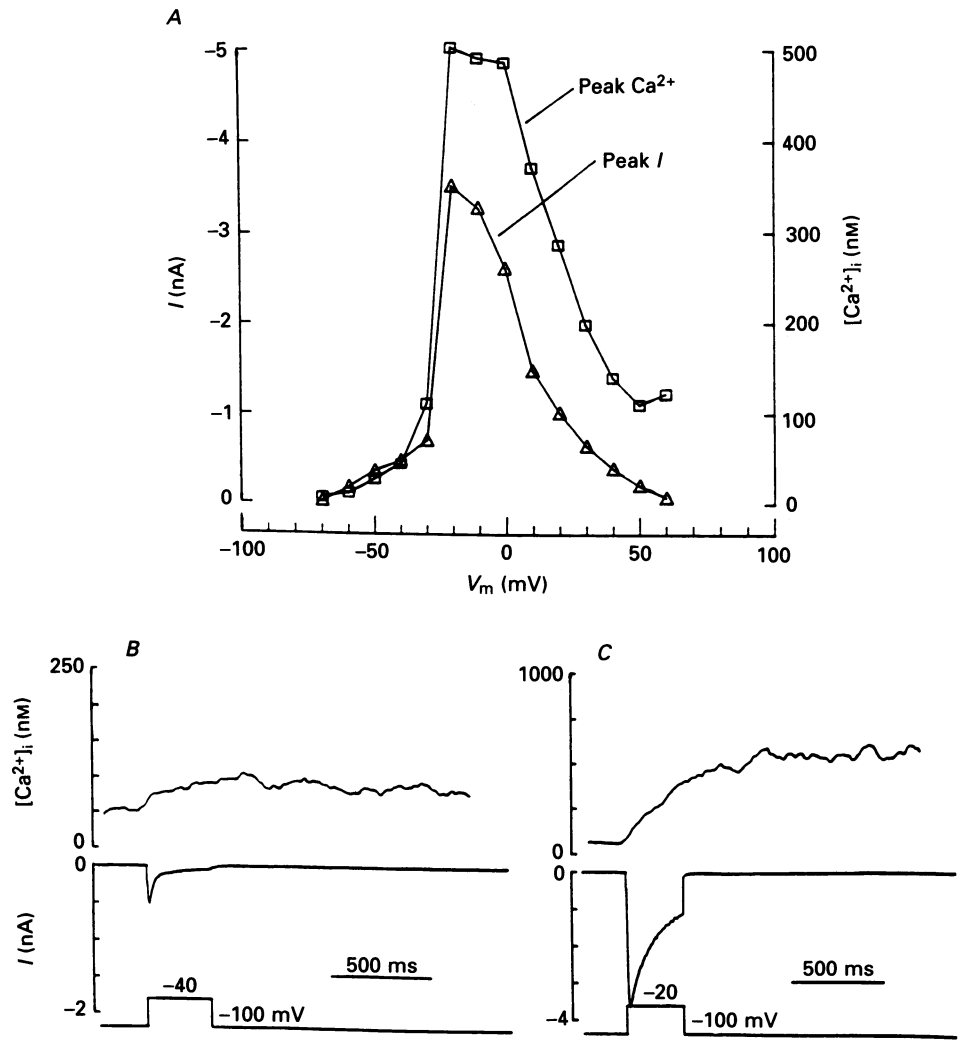

Fig. 3. The I_{Ca} and $[Ca^{2+}]_i$ *versus* voltage relationship for a DRG neurone. *A*, the cell was held at −100 mV and stepped to the test potentials indicated for 320 ms. Leak was corrected as described in Methods. *B*, individual sweep showing the small transient T-type current and $[Ca^{2+}]_i$ transient elicited from a depolarizing step to −40 mV, *C*, individual sweep showing the large I_{Ca} and $[Ca^{2+}]_i$ transient elicited from a depolarizing step to −20 mV. Note that 100 μM-Fura-2 was the only Ca^{2+} chelator present in the pipette solution.

long test pulses is considered. However, in Fig. 5*B* where the peak $[Ca^{2+}]_i$ values are plotted *versus* the total amount of charge flowing across the membrane, all three sets of data from Fig. 5*A* are superimposed, consistent with the idea that larger Ca^{2+} loads were more heavily buffered than smaller loads. Thus large Ca^{2+} loads could not elevate the $[Ca^{2+}]_i$ above a 'ceiling' maintained by a buffering mechanism with

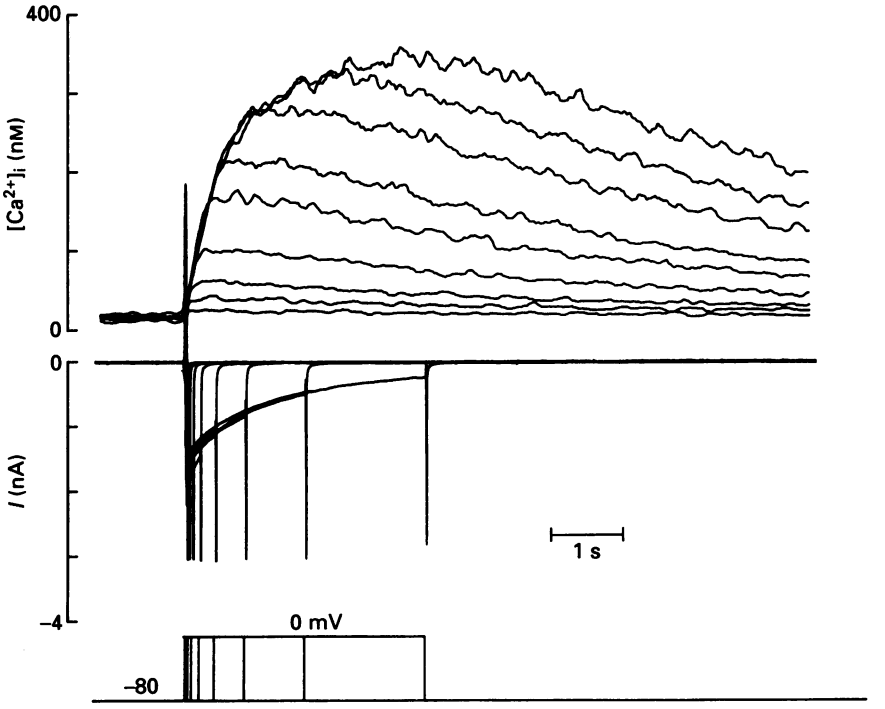

Fig. 4. $[Ca^{2+}]_i$ transient and I_{Ca} were varied by applying test pulses of different durations. Nine sweeps are superimposed displaying recordings from a cell held at −80 mV and depolarized to 0 mV for 10, 20, 40, 80, 160, 320, 640, 1280 and 2560 ms. These data were collected in an extracellular $[Ca^{2+}]$ of 1 mM.

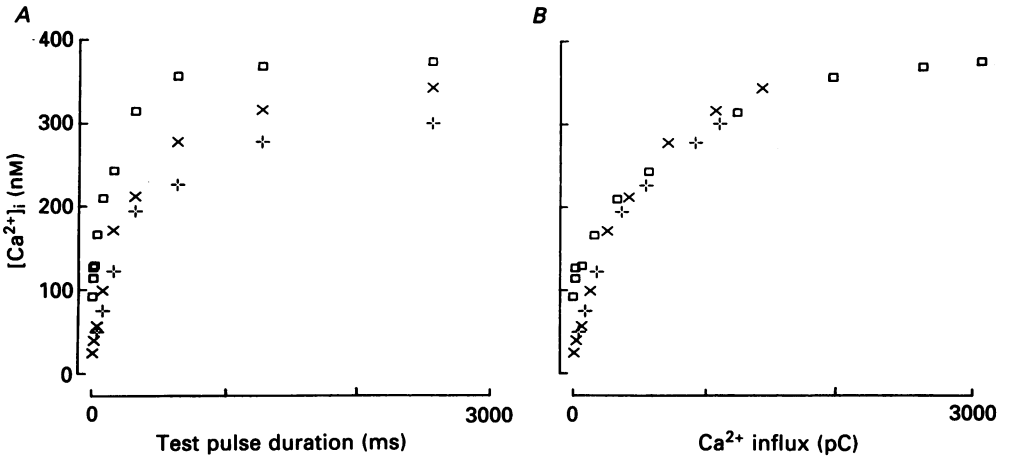

Fig. 5. Plots of test pulse duration and Ca^{2+} influx *versus* $[Ca^{2+}]_i$. *A*, the duration of the test pulse is plotted *versus* the peak of the $[Ca^{2+}]_i$ transient that resulted from a depolarization to 0 mV from a holding potential of −80 mV. The data were all recorded from the cell shown in Fig. 4. Data were recorded in an external $[Ca^{2+}]$ of 1 mM (displayed in Fig. 4, ×), 10 mM (□) or 1 mM after Ca^{2+} channel run-down (+). *B*, the data displayed in *A* are re-plotted *versus* the integral of the inward current during the test pulse.

sufficient capacity to remain unsaturated even when challenged with large Ca^{2+} loads. The asymptotic relationship between integrated I_{Ca} and $[Ca^{2+}]_i$ was seen in 75% of the cells studied ($n = 40$). Those cells which displayed a linear relationship had small current-to-cell-volume ratios and thus presumably would have approached an asymptote had a large enough Ca^{2+} load been applied. Thus as the $[Ca^{2+}]_i$ reaches

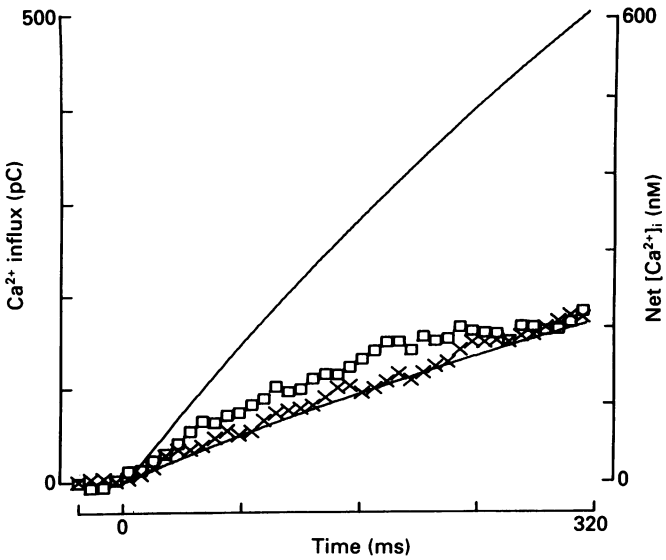

Fig. 6. The $[Ca^{2+}]_i$ is no longer proportional to Ca^{2+} influx for large Ca^{2+} loads. The plot is the same format as Fig. 2*A* and is of selected records from Fig. 5. The continuous lines represent the integral of the I_{Ca} during the 320 ms test pulse and the symbols represent the $[Ca^{2+}]_i$ calculated for a 320 ms test pulse in 1 mM-external Ca^{2+} (×) or 10 mM-external Ca^{2+} (□). Data were scaled to superimpose the smaller current and $[Ca^{2+}]_i$ values.

higher levels the Ca^{2+} buffering rate increases presumably either due to the more complete activation of Ca^{2+}-dependent processes or to the recruitment of additional low-affinity buffering mechanisms. This finding is consistent with the increase in Ca^{2+} buffering capacity measured at higher $[Ca^{2+}]_i$ levels in molluscan neurones (Ahmed & Connor, 1988). The observation that a smaller percentage of large Ca^{2+} loads remains free in the cytoplasm relative to smaller loads can also be observed when the integral of the I_{Ca} is compared to the resulting $[Ca^{2+}]_i$ transient in each case. In Fig. 6 these two parameters are plotted during a 320 ms test pulse for the data generated in the presence of either 10 or 1 mM-extracellular Ca^{2+} (□ and ×, respectively). Clearly the total Ca^{2+} influx is much greater in higher extracellular Ca^{2+} yet the magnitude of the $[Ca^{2+}]_i$ transients for the two sweeps are quite similar.

$[Ca^{2+}]_i$ buffering in molluscan neurones has been shown to be dependent on the duration of Ca^{2+} influx (Ahmed & Connor, 1986). To determine whether the asymptotic relationship between Ca^{2+} influx and $[Ca^{2+}]_i$ was dependent on the method of introducing Ca^{2+} load to the cell we varied the Ca^{2+} load presented to three

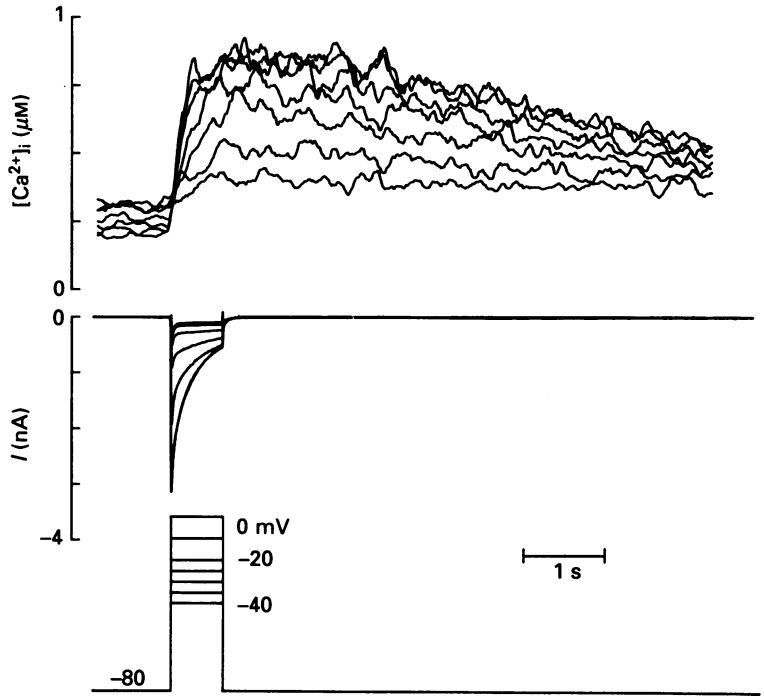

Fig. 7. $[Ca^{2+}]_i$ transient and I_{Ca} were varied by applying test pulses to different potentials. Seven sweeps are superimposed displaying recordings from a cell held at −80 mV and depolarized to −40, −35, −30, −25, −20, −10 and 0 mV for 640 ms. These recordings were made in an extracellular $[Ca^{2+}]$ of 2 mM.

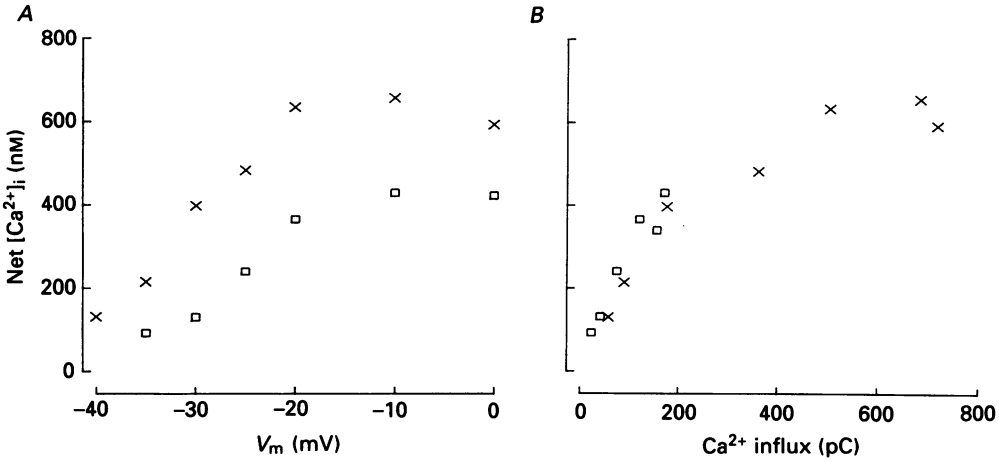

Fig. 8. Plots of test pulse potential and Ca^{2+} influx *versus* $[Ca^{2+}]_i$. *A*, the test pulse potential is plotted *versus* the peak of the $[Ca^{2+}]_i$ transient that resulted from a 640 (×) or 160 ms (□) depolarization. The data were recorded from the cell shown in Fig. 7. *B*, the data displayed in *A* are re-plotted *versus* the integral of the current during the test pulse.

neurones by varying the test potential while keeping the test pulse duration constant. Seven sweeps displaying I_{Ca} and $[Ca^{2+}]_i$ recordings elicited by 640 ms test pulses stepping from a holding potential of −80 mV to test potentials ranging from −40 to 0 mV are superimposed in Fig. 7. Figure 8*A* illustrates the relationship between test potential and the peak of the $[Ca^{2+}]_i$ transient elicited for the records displayed in Fig. 7 as well as for data recorded from the same cell at the shorter test

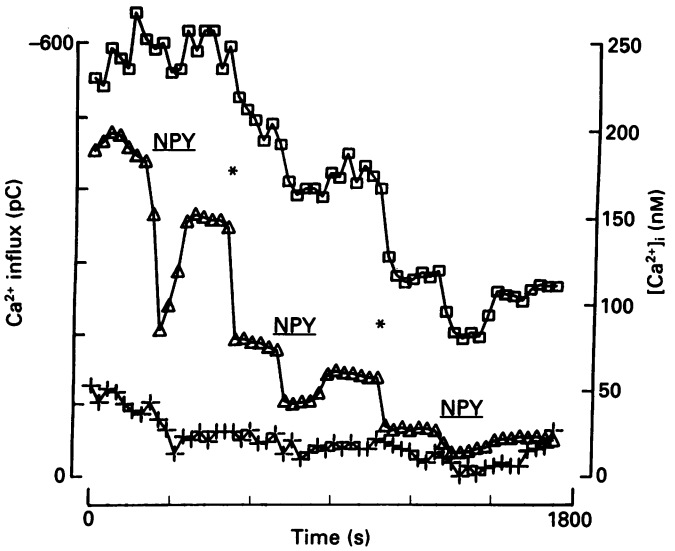

Fig. 9. Neuropeptide Y inhibition of the $[Ca^{2+}]_i$ transient is dependent on the size of the Ca^{2+} load applied to the cell. The cell was voltage clamped to −80 mV in the whole-cell configuration and depolarized to 0 mV every 20 s. The integral of the resulting I_{Ca} (△) and the peak (□) and basal (+) $[Ca^{2+}]_i$ levels are plotted for each sweep. At the time indicated by the horizontal bars 100 nM-NPY was superfused onto the cell. Initially the test pulse duration was 320 ms and at the times indicated by the asterisks the test pulse duration was reduced by one-half, to 160 and 80 ms respectively.

pulse duration of 160 ms. Note that the curve generated from the 640 ms pulses reaches a half-maximal $[Ca^{2+}]_i$ at a more hyperpolarized potential than the curve generated from 160 ms pulses. This suggests that, as described above for long test pulses, large Ca^{2+} loads are more efficiently buffered than smaller loads. Indeed when the data are plotted as the integral of the I_{Ca} *versus* the peak of the $[Ca^{2+}]_i$ transient (Fig. 8*B*) it is clear that when large Ca^{2+} loads are applied to the cell the $[Ca^{2+}]_i$ approaches an asymptote.

The observation that large Ca^{2+} loads are more efficiently buffered than small loads may be of considerable importance to the understanding of the regulation of $[Ca^{2+}]_i$ signals as a result of the modulation of Ca^{2+} channels during neurotransmission. For example in Fig. 9 the ability of neuropeptide Y to modulate $[Ca^{2+}]_i$ transients is shown to be dependent on the size of the Ca^{2+} load applied to the cell. In this figure

the basal $[Ca^{2+}]_i$, the integral of the I_{Ca} and the peak of the $[Ca^{2+}]_i$ transient from a series of sweeps generated every 20 s are plotted. Note that initially all three parameters were stable. At time 225 s, 100 nM-NPY was superfused onto the cell. This peptide has been previously shown to be an effective inhibitor of voltage-sensitive Ca^{2+} channels in these neurones (Ewald, Sternweis & Miller, 1988).

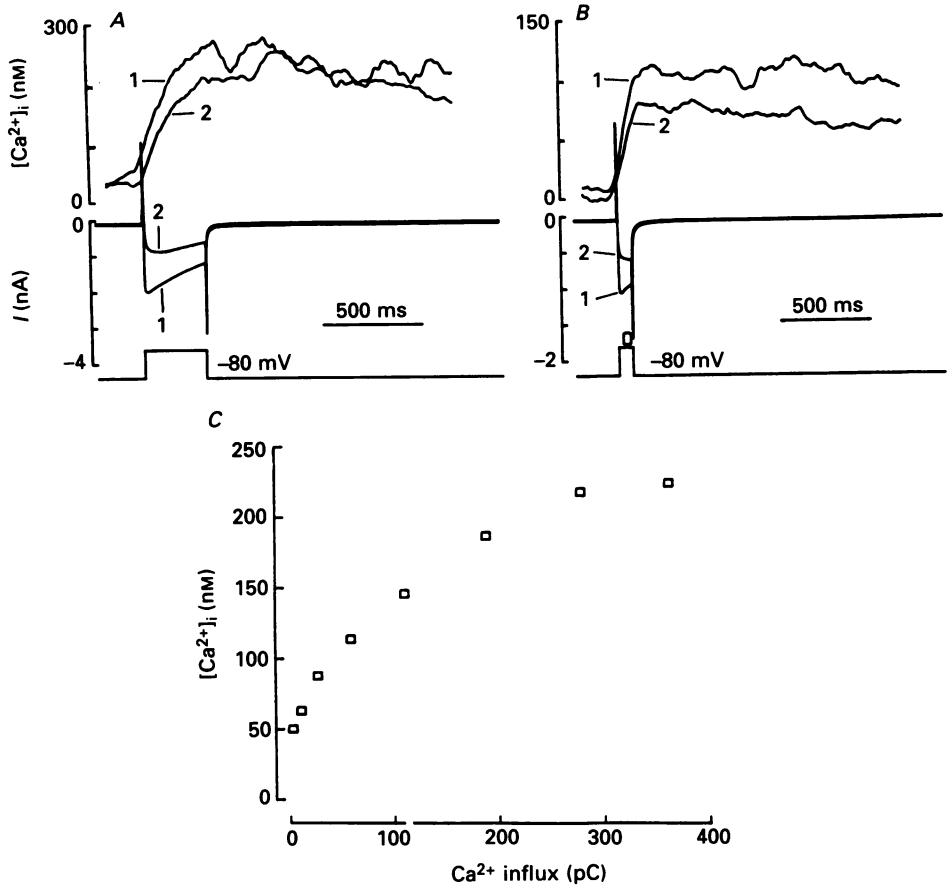

Fig. 10. Selected plot and records for the experiment described in Fig. 9. *A*, superimposed sweeps prior to (1) and during (2) the first exposure of the cell to NPY. *B*, superimposed sweeps prior to (1) and during (2) the third exposure of the cell to NPY. *C*, Ca^{2+} influx *versus* $[Ca^{2+}]_i$ curve for the same cell described above. The curve was generated by applying depolarizing test pulses for 20, 40, 80, 160, 320, 640, 1280 and 2560 ms duration following the time course displayed in Fig. 9.

Consistent with its action on Ca^{2+} channels, perfusion of the peptide onto the cell resulted in a large decrease in the inward I_{Ca}. Surprisingly, the peak magnitude of the $[Ca^{2+}]_i$ transient was not reduced, suggesting that the I_{Ca} was of sufficient magnitude for the Ca^{2+} influx–$[Ca^{2+}]_i$ relationship to be at the asymptotic portion of the curve (see Fig. 10*C*). The representative sweeps in Fig. 10*A* show clearly that the inward current was markedly inhibited by the peptide yet it produced little effect on the

$[Ca^{2+}]_i$ transient. In some sweeps, such as the one displayed in Fig. 10*A*, the time to reach the peak of the $[Ca^{2+}]_i$ transient was increased. However, this was not a consistent finding. The test pulse duration was then shortened (at the time indicated by the asterisks in Fig. 9) to 160 ms to decrease the Ca^{2+} load placed on the neurone. The peptide was reapplied (at time = 700 s) and again a significant inhibition of the I_{Ca} resulted. This exposure produced a slight inhibition of the $[Ca^{2+}]_i$ transient as well. The test pulse duration was then shortened to 80 ms and once again the cell was exposed to NPY (time = 1325 s). This treatment produced a similar inhibition of the I_{Ca} but also produced a proportionally much larger inhibition of the $[Ca^{2+}]_i$ transient. In Fig. 10*B* the peak current was reduced by 47%, similar to the 53% inhibition seen in Fig. 10*A*, but in this case the $[Ca^{2+}]_i$ transient was inhibited by 31% *versus* no effect for the longer pulses. Figure 10*C* displays the Ca^{2+} influx–$[Ca^{2+}]_i$ relationship for this same cell determined after the final neuropeptide exposure. Clearly the long 320 ms test pulses were producing inward Ca^{2+} fluxes and peak $[Ca^{2+}]_i$ values corresponding to the asymptotic portion of the curve. This experiment is representative of four replicates in which NPY proved more effective in reducing the peak of the $[Ca^{2+}]_i$ transients resulting from small Ca^{2+} loads relative to larger loads.

The relationship between action potential frequency and $[Ca^{2+}]_i$

We wished to determine whether the saturation phenomenon described so far could also be produced when Ca^{2+} influx was associated with action potential generation. When cells were held in whole-cell current clamp brief current injections elicited action potentials. Eliciting a single action potential produced a small but long-lasting increase in $[Ca^{2+}]_i$ (Fig. 11*A*). Firing several action potentials in rapid succession produced a stepwise increase in the $[Ca^{2+}]_i$ (Fig. 11*B*). In the presence of 1 mM-4-aminopyridine high-frequency bursts of action potentials could be elicited as shown in Fig. 11*C–E*. The relationship between the number of action potentials in a burst and the resulting increase in $[Ca^{2+}]_i$ would be predicted to approach an asymptote based on the data presented in Figs 7, 9 and 10*C*. This was found to be true as illustrated in Fig. 11*F*. Thus it appears that the Ca^{2+} loads applied in the whole-cell voltage clamp are reasonable approximations for loads resulting from high-frequency bursts of action potentials. By analogy with the results presented in Figs 9 and 10, modulation of $[Ca^{2+}]_i$ increases produced by neurotransmitters in response to cell firing might be expected to be a frequency-dependent phenomenon (see Discussion).

Mitochondrial buffering of large Ca^{2+} *loads*

We next conducted experiments designed to investigate the nature of the cellular mechanisms involved in buffering Ca^{2+} loads in DRG neurones. The ability of isolated mitochondria to sequester large amounts of Ca^{2+} *in vitro* suggests that this organelle may play a role in the regulation of $[Ca^{2+}]_i$ *in vivo* (Nicholls, 1978, 1985). However, it has not been clear whether mitochondria normally participate in Ca^{2+} buffering *in situ* under normal physiological conditions or only when $[Ca^{2+}]_i$ reaches abnormally high levels under pathological circumstances (Carafoli, 1987). That mitochondria are capable of buffering $[Ca^{2+}]_i$ in intact neurones is demonstrated in the experiments illustrated in Fig. 12.

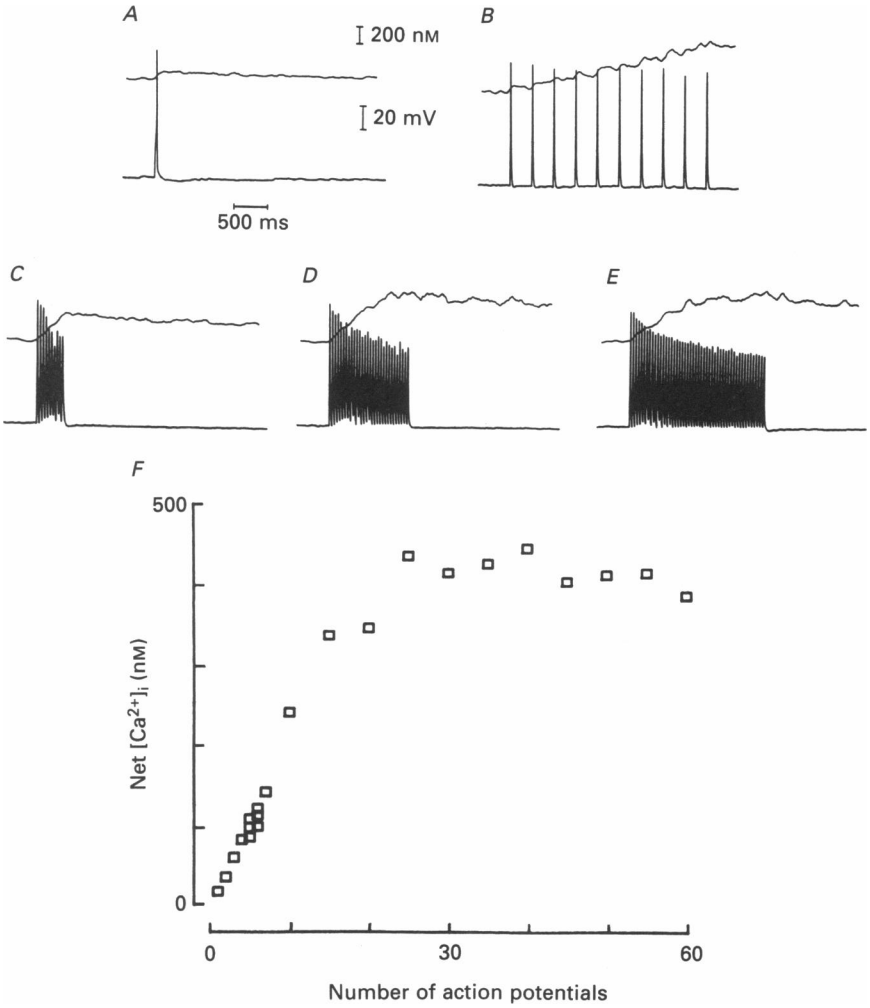

Fig. 11. Simultaneous current-clamp and $[Ca^{2+}]_i$ recordings from DRG neurones. *A*, injection of 150 pA for 32 ms elicited a single action potential in this DRG neurone that resulted in a small but sustained elevation in $[Ca^{2+}]_i$. *B*, ten current injections of 700 pA for 16 ms resulted in a stepwise increase in $[Ca^{2+}]_i$. Ten (*C*), thirty (*D*) or fifty (*E*) injections of 700 pA for 16 ms were applied to a single DRG neurone every 40 ms. *F*, a number of stimuli ranging from one to sixty current injections were applied to the cell shown in *C–E* and the resulting increase in $[Ca^{2+}]_i$ is plotted *versus* the number of action potentials fired. *B–E* are from the same cell and are in the presence of 1 mM-4-aminopyridine.

Dorsal root ganglion neurones were loaded with Fura-2 using the esterified form of the dye as described in Methods. The experiments described in Fig. 12 were performed on intact cells that were not voltage clamped. Cells were loaded with Ca^{2+} by activation of voltage-sensitive Ca^{2+} channels in response to superfusion with a 50 mM-K^+ depolarizing solution. We have previously reported that 50 mM-K^+-induced depolarization of DRG neurones produces a $[Ca^{2+}]_i$ transient that is unique

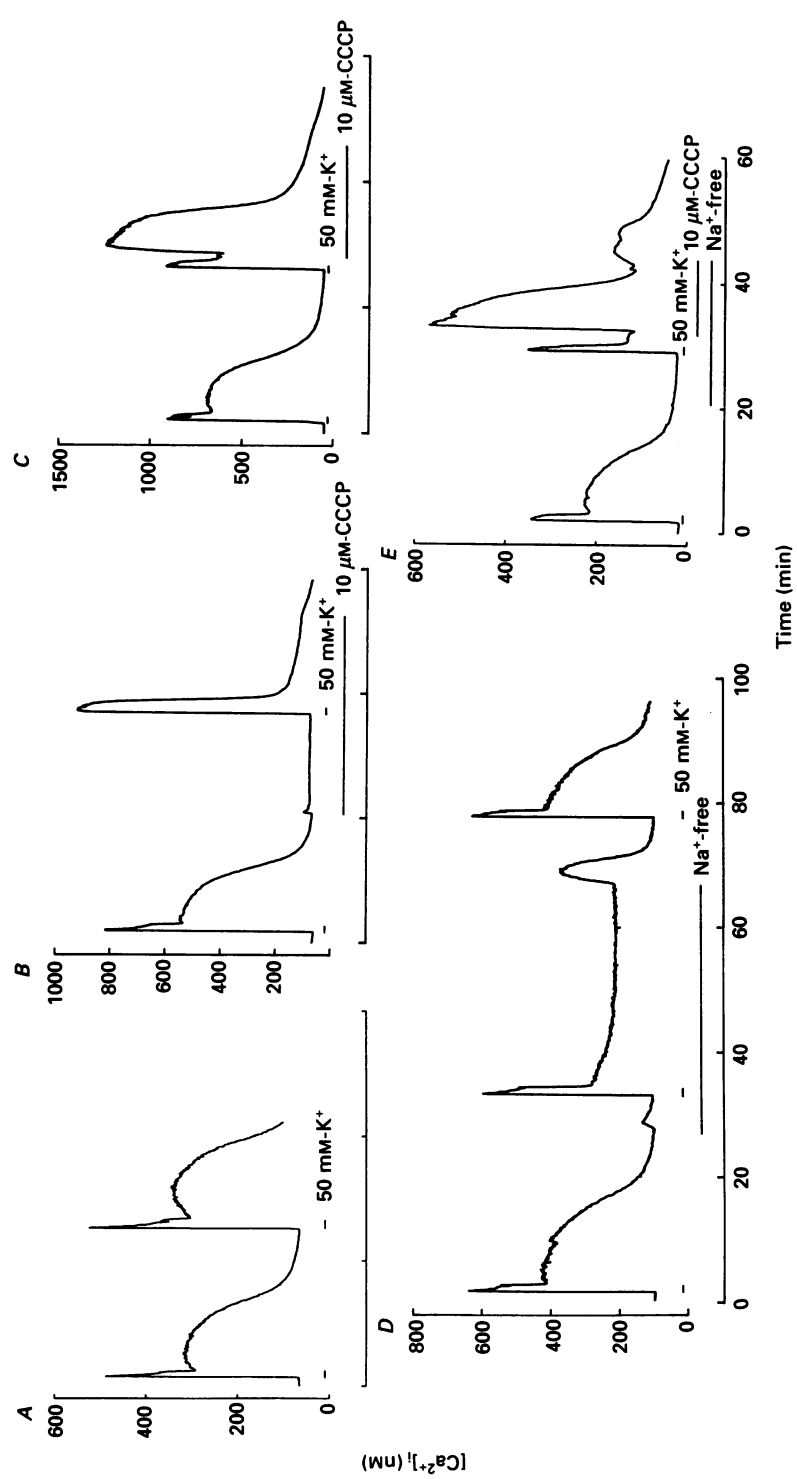

Fig. 12. Mitochondrial buffering of large Ca^{2+} loads. *A*, drug-free control response demonstrating reproducible $[Ca^{2+}]_i$ transients in response to depolarization induced by superfusion with 50 mM-K^+ for 2 min. K^+ was exchanged for Na^+ reciprocally. All additions to the media are indicated by the horizontal bars. *B*, following an initial control response to 50 mM-K^+ the cell was superfused with 10 μM-CCCP and subsequently re-stimulated with high K^+. *C*, following an initial control response and a second 50 mM-K^+ stimulus 1 μM-CCCP was applied to the cell during the plateau phase of the transient as indicated by the horizontal bar. *D*, following an initial control response to 50 mM-K^+ the cell was superfused with media in which all Na^+ had been replaced with *N*-methyl-D-glucamine. The cell was then re-stimulated and the sustained plateau finally terminated by the re-addition of Na^+ to the medium. A subsequent high-K^+ stimulus confirmed recovery of the cell. *E*, following initial control and Na^+-free, high-K^+ responses CCCP was superfused onto the cell during the plateau phase of the $[Ca^{2+}]_i$ transient as indicated by the horizontal bar.

in form to recordings from the cell bodies of these cells (Thayer *et al.* 1988*b*, *c*). The response is characterized by a rapid elevation in $[Ca^{2+}]_i$ from a resting level of 92 ± 5 nM to a peak level of 731 ± 56 nM ($n = 87$) followed by a rapid relaxation in $[Ca^{2+}]_i$ upon removal of the stimulus to a sustained plateau $[Ca^{2+}]_i$ level which varied in magnitude considerably among cells but remained very reproducible for an individual cell. This plateau or 'tail' may last as long as 45 min. The average response duration was quantified by measuring the width of the transient at 25% of the peak $[Ca^{2+}]_i$ reached (full-width 1/4 maximum, 'FWQM') which was $10{\cdot}8 \pm 0{\cdot}7$ min for a 2 min depolarizing stimulus. An example of depolarization-induced $[Ca^{2+}]_i$ transients in DRG neurones is shown in Fig. 12*A*. These $[Ca^{2+}]_i$ transients were very reproducible for a given cell with the peak height, plateau level and duration of the response remaining relatively constant in response to repeated stimuli. In nineteen experiments the second response decreased only slightly in magnitude to 89 ± 5% of the first response. The duration of the transient was also slightly reduced with the recovery time 88 ± 5% (FWQM) of the first response.

Mitochondria sequester Ca^{2+} by an energy-dependent mechanism which is driven by the large pH gradient across the inner mitochondrial membrane. Thus agents which collapse the mitochondrial H^+ gradient such as uncouplers of oxidative phosphorylation should release mitochondrial Ca^{2+} stores into the cytoplasm and compromise the ability of mitochondria to sequester additional Ca^{2+}. In the experiment described in Fig. 12*B*, after an initial control response, the mitochondrial uncoupling agent carbonyl cyanide *m*-chlorophenyl-hydrazone (CCCP) was superfused onto the cell. The metabolic poison was applied while the $[Ca^{2+}]_i$ was at a resting level. The small change in cytosolic $[Ca^{2+}]$ produced by the uncoupler indicates that little Ca^{2+} was sequestered in the mitochondria while $[Ca^{2+}]_i$ was at a basal level. This finding is consistent with the relatively low affinity of the mitochondrial Ca^{2+} uptake process. However, the depolarization-induced $[Ca^{2+}]_i$ transient was markedly changed in the presence of the uncoupler. The initial phase of the $[Ca^{2+}]_i$ transient reached a higher peak $[Ca^{2+}]_i$ (924, 601, 362 nM) value than the preceding control response (817, 454, 242 nM, respectively), increasing by 36 ± 12% ($n = 3$). In contrast the duration of the slowly buffered Ca^{2+} tail was decreased dramatically (79 ± 1% inhibition), suggesting that mitochondrial Ca^{2+} cycling may play a role in maintaining the plateau phase of the transient. Indeed when the CCCP was applied during the plateau phase of the response (Fig. 12*C*) a large increase in $[Ca^{2+}]_i$ resulted, indicating that the mitochondria had sequestered a large amount of Ca^{2+} ($n = 8$). Also note that the durations of the control and CCCP-treated responses in Fig. 12*C* were similar. This suggests that the process which ultimately removes Ca^{2+} from the cytoplasm was working at the same rate during both responses. The similar duration of the two responses as well as the absence of a significant amount of Ca^{2+} in mitochondria under resting conditions are consistent with the mitochondria playing a buffering role in which they act as a sink for Ca^{2+}, sequestering it when the $[Ca^{2+}]_i$ is above a certain 'set-point' (Nicholls, 1985) and releasing it when the $[Ca^{2+}]$ is below the set-point. Thus in the $[Ca^{2+}]_i$ transients described here the mitochondria sequester Ca^{2+} during the initial phase of the response buffering the $[Ca^{2+}]_i$ down to the plateau level which is presumably the mitochondrial Ca^{2+} set-point. Slower $[Ca^{2+}]_i$ buffering processes continue to pump Ca^{2+} into other organelles or out of the

cell during the plateau phase, while the mitochondria release Ca^{2+} into the cytoplasm at a rate equal to the pump's rate of Ca^{2+} removal from the cytoplasm. Eventually the mitochondrial store of Ca^{2+} is depleted and the $[Ca^{2+}]_i$ is buffered down to basal levels.

Mitochondria release Ca^{2+} by means of a Na^+-dependent process (Gunter, Wingrove, Banerjee & Gunter, 1988). Thus decreasing the cytosolic $[Na^+]$ will decrease the rate of efflux of Ca^{2+} from mitochondria having the net effect of increasing the mitochondrial affinity for Ca^{2+} and decreasing the $[Ca^{2+}]$ set-point. In agreement with this finding, which was based on studies with isolated mitochondria, the experiment illustrated in Fig. 12*D* shows that removing extracellular Na^+ decreases the level of the plateau by $35 \pm 8\%$ from 259 ± 25 nM in the control to 190 ± 20 nM in the absence of Na^+ ($n = 7$). Note that the duration of the plateau in the absence of Na^+ is considerably longer than the control response indicating that the pumps which ultimately remove Ca^{2+} from the cytoplasm are working below their capacity, presumably because their rate is dependent on the $[Ca^{2+}]_i$. The contribution of extracellular Na^+ to Ca^{2+} buffering will be discussed in a subsequent section. Figure 12*E* illustrates an experiment which confirms that the mitochondria are indeed loaded with Ca^{2+} during the low set-point plateau seen in decreased Na^+. Application of CCCP during the reduced plateau levels produced a large release of mitochondrial Ca^{2+} ($n = 5$).

The presence of this Ca^{2+} tail in DRG neurone $[Ca^{2+}]_i$ transients suggests that modulation of $[Ca^{2+}]_i$ by the regulation of Ca^{2+} influx through Ca^{2+} channels might modulate the duration of the response as well as its amplitude. Indeed superfusion of DRG neurones with either NPY, which acts via its receptor and a G-protein to inhibit Ca^{2+} channels (Ewald *et al.* 1988), or the dihydropyridine Ca^{2+} channel antagonist nitrendipine (NIT) produced a dramatic shortening in the duration of the $[Ca^{2+}]_i$ transient in DRG neurone cell bodies (Fig. 13*A* and *B*). One micromolar NIT decreased the duration of the plateau (FWQM) by $76 \pm 16\%$ ($n = 9$). At 100 nM NPY inhibited the duration of the $[Ca^{2+}]_i$ transient by $50 \pm 16\%$ ($n = 6$). These findings are consistent with the idea that the decreased Ca^{2+} influx through Ca^{2+} channels results in a similarly reduced load of Ca^{2+} stored in the mitochondria, corresponding to a shortening of the duration of the $[Ca^{2+}]_i$ transient.

We have previously demonstrated that in contrast to the depolarization-induced $[Ca^{2+}]_i$ transients recorded in the cell bodies of DRG neurones, recordings made from the processes of these same cells appear markedly different (Thayer *et al.* 1988*c*; Fig. 13*C*). Fifty millimolar K^+-induced $[Ca^{2+}]_i$ transients in DRG processes were smaller than those recorded from cell bodies reaching an average peak $[Ca^{2+}]_i$ of 576 ± 94 nM from a similar resting level of 121 ± 14 nM ($n = 19$). However, the most striking difference was the greatly reduced time required to recover to basal levels after removal of the depolarizing stimulus. The duration of the transients in processes was (FWQM) $2{\cdot}9 \pm 0{\cdot}3$ min, only 27% of the duration of $[Ca^{2+}]_i$ transients in the soma. This more rapid recovery is probably not due to a reduced Ca^{2+} load in the processes as might be suggested by the lower peak $[Ca^{2+}]_i$ levels, since no correlation between peak height and duration was observed. Note also that the 2 min stimulus period is included in the duration measurement so that the rate of recovery of $[Ca^{2+}]_i$ in the processes is less than 1 min and approaches the time resolution of the superfusion

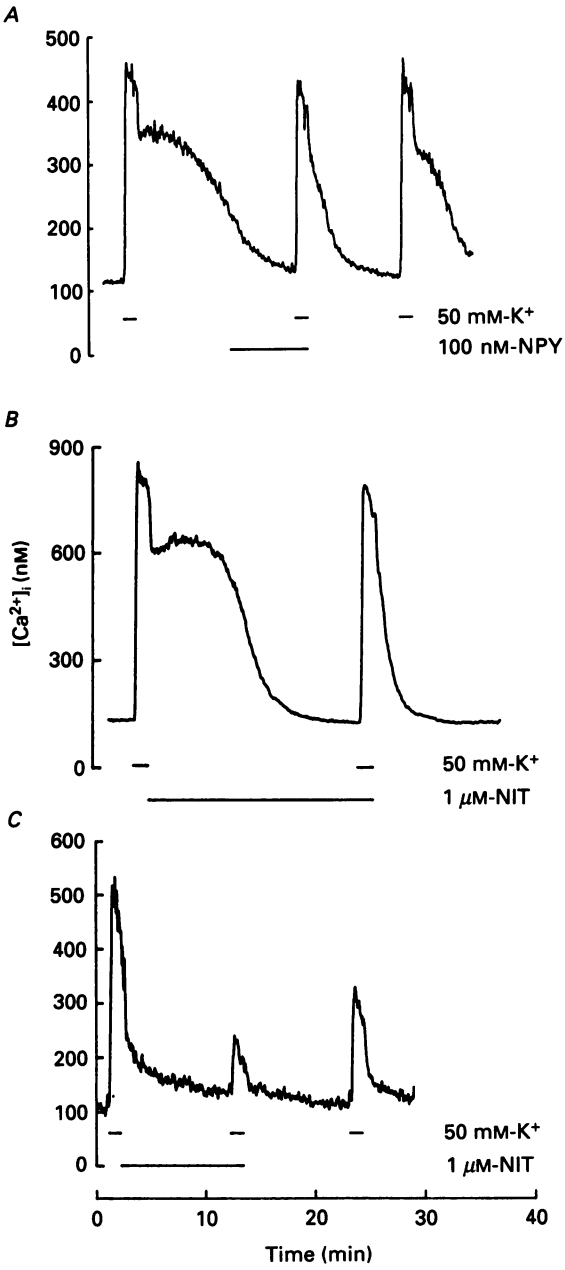

Fig. 13. Inhibition of depolarization-induced $[Ca^{2+}]_i$ transients by NIT and NPY in DRG cell bodies and processes. $[Ca^{2+}]_i$ transients were elicited by superfusion with 50 mM-K^+ for 2 min. Additions to the bathing solution are indicated by the horizontal bars. *A*, following an initial control response 100 nM-NPY was superfused onto a DRG cell soma and re-stimulated with 50 mM-K^+. *B*, following an initial control response 1 μM-NIT was superfused onto a DRG cell soma and re-stimulated with 50 mM-K^+. *C*, following an initial control response 1 μM-NIT was superfused onto a DRG cell process and re-stimulated with 50 mM-K^+.

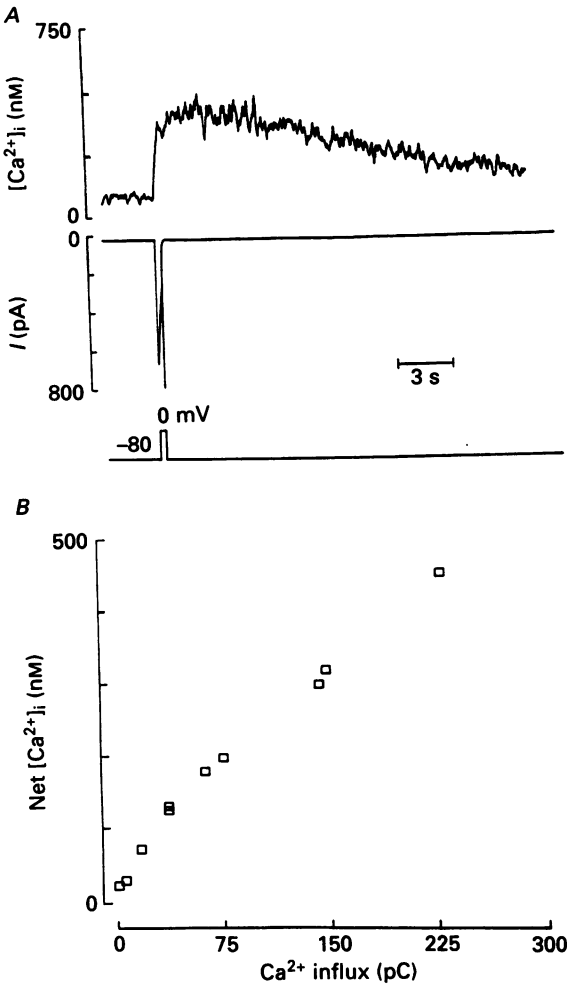

Fig. 14. Ruthenium Red removes a high-capacity Ca^{2+} buffering component of depolarization-induced $[Ca^{2+}]_i$ transients. *A*, simultaneous I_{Ca} and $[Ca^{2+}]_i$ recording from a DRG neurone with 10 μM-Ruthenium Red in the patch pipette. The cell was depolarized to 0 mV for 320 ms from a holding potential of −80 mV. *B*, in the presence of Ruthenium Red the relationship between Ca^{2+} influx and $[Ca^{2+}]_i$ was linear even for large Ca^{2+} loads. The curve was generated by applying depolarizing test pulses for 10, 20, 40, 80, 160, 320, 640, 1280 and 2560 ms duration.

apparatus. Inhibition of Ca^{2+} influx in DRG processes by NIT resulted in a decreased amplitude of the $[Ca^{2+}]_i$ transient without the shortening in the duration of the signal as observed in cell bodies (Fig. 13*C*). Nitrendipine reduced the peak of the $[Ca^{2+}]_i$ transient by $67 \pm 3\%$ ($P < 0{\cdot}001$, paired t test, $n = 6$) but reduction in the duration was not statistically significant. It is evident that both the processes and cell bodies of these neurones possess Ca^{2+} channels which are sensitive to dihydropyridines. However, the Ca^{2+} load induced by activation of these channels is presumably buffered by a different mechanism in the two parts of the cell.

Mitochondria in the cell body appear to play a role in buffering the $[Ca^{2+}]_i$ transients elicited by relatively brief depolarizations such as voltage steps in whole-cell patch-clamp experiments as well. In contrast to the cell superfusion experiments addition of 10 μM-CCCP to cells in the whole-cell configuration of the patch clamp produced a large (> 2 μM) increase in $[Ca^{2+}]_i$ ($n = 15$). Thus it appears that the mitochondria have accumulated Ca^{2+} during establishment of the whole-cell clamp presumably during transition from the cell-attached to the whole-cell configuration. The more frequent application of depolarizing stimuli and the ionic leak at the pipette seal could also contribute to the somewhat higher resting $[Ca^{2+}]_i$ levels seen in whole-cell patch-clamp experiments. Cells in the whole-cell voltage clamp rarely recovered from treatment with CCCP and those that did (three of fifteen) had greatly diminished I_{Ca} (data not shown). Thus another mitochondrial Ca^{2+} uptake inhibitor was employed in patch-clamp experiments. Ruthenium Red has been shown to be an effective inhibitor of mitochondrial Ca^{2+} uptake *in vitro* (Moore, 1971). At the concentrations used in these experiments this compound does not significantly quench the fluorescence of Fura-2. Ruthenium Red is membrane impermeable and thus was ineffective in superfusion experiments ($n = 3$). However, when introduced into the patch pipette 10 μM-Ruthenium Red significantly altered the $[Ca^{2+}]_i$ buffering properties of DRG neurones. Figure 14*A* illustrates the $[Ca^{2+}]_i$ transient elicited in a cell dialysed with Ruthenium Red. Removal of the mitochondrial Ca^{2+}-buffering component changed the relationship between Ca^{2+} influx and the resulting peak of the $[Ca^{2+}]_i$ transient (Fig. 14*B*). Presenting the cell with increasing Ca^{2+} loads no longer produced an increase in $[Ca^{2+}]_i$ that approached an asymptote ($n = 4$). This linear relationship was observed with Ca^{2+} loads as high as 1000 pC in Ruthenium Red-treated cells suggesting that even large Ca^{2+} loads fail to produce an asymptote. This result is consistent with the idea that the low-affinity, high-capacity, mitochondrial Ca^{2+} buffering system plays a more significant role in buffering large Ca^{2+} loads. It is also of interest to note that the $[Ca^{2+}]_i$ limit to which the peak of the $[Ca^{2+}]_i$ transient approaches with large Ca^{2+} loads in Figs 5*B*, 8*B* and 10*C* is within the range of the plateau phase of high-K^+-induced $[Ca^{2+}]_i$ transients described in Figs 12 and 13, suggesting that both the asymptote and the plateau are determined by the mitochondrial Ca^{2+}-buffering set-point.

Na^+ and ATP dependence of $[Ca^{2+}]_i$ buffering

We investigated the possible role of energy-dependent pumps, such as the Ca^{2+}–Mg^{2+}-ATPase and also the Na_o^+–Ca_i^{2+} exchanger, as contributors to $[Ca^{2+}]_i$ buffering in DRG neurones. In contrast to studies on squid axon and rat brain synaptosomes (Allen & Baker, 1986; Sanchez-Armass & Blaustein, 1987) but in agreement with studies on frog sympathetic neurones (Nohmi & Kuba, 1984), *Aplysia* bag cells (Levy & Tillotson, 1988) and rat DRG neurones (Benham, Evans & McBain, 1989) we could not demonstrate any effect of the extracellular $[Na^+]$ on the $[Ca^{2+}]_i$ transient. Figure 15 illustrates $[Ca^{2+}]_i$ transients elicited from long (640 ms) and short (80 ms) stimuli. Two traces are shown for each stimulus. One of these is in the presence of physiological concentrations of Na^+ and the other is under conditions in which all extracellular Na^+ has been replaced with TEA^+. Clearly removal of extracellular Na^+ did not affect the $[Ca^{2+}]_i$ transient in this cell which is

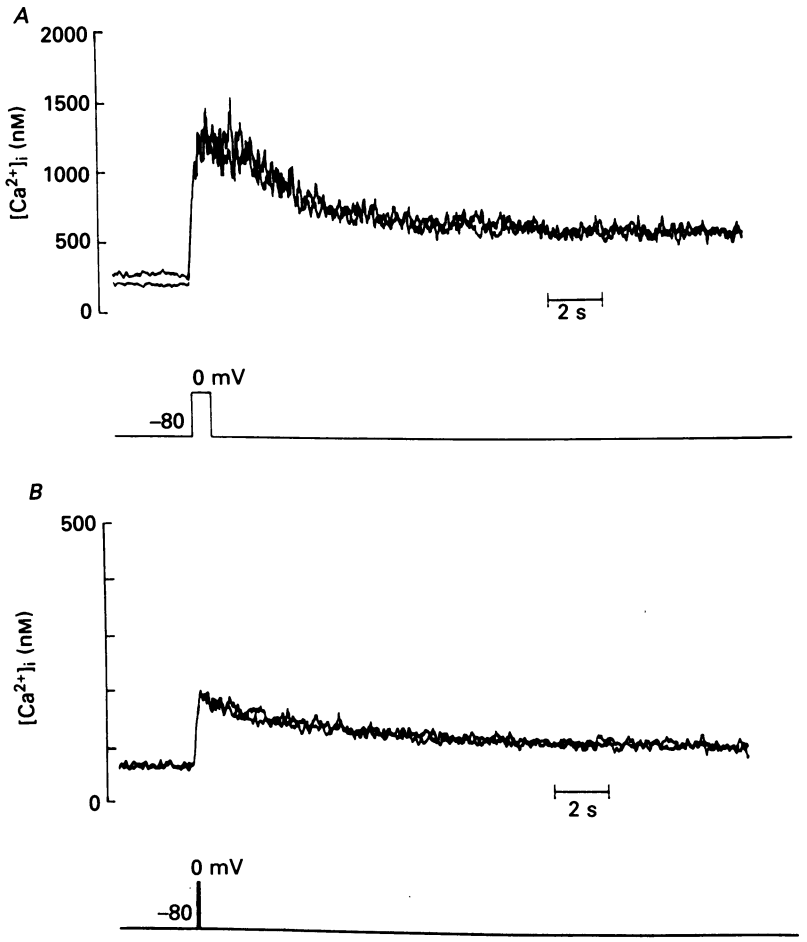

Fig. 15. Depolarization-induced $[Ca^{2+}]_i$ transients in DRG neurones elicited in the absence of extracellular Na^{2+}. *A*, a DRG neurone was held at −80 mV and depolarized to 0 mV for 640 ms in the presence and absence of extracellular Na^+. TEA^+ was substituted for Na^+ reciprocally. *B*, the same cell was held at −80 mV and depolarized to 0 mV for 80 ms in the absence and presence of extracellular Na^+.

representative of fifteen replicate experiments. Additionally, this experiment demonstrates that there is no deleterious effect of TEA^+ substitution for external Na^+ as has been suggested in other systems (Zucker, 1981). While removal of extracellular Na^+ did not alter the $[Ca^{2+}]_i$ transient, occasionally a small change in the basal $[Ca^{2+}]_i$ was seen (Fig. 15*A*). This effect was transient and variable (see also Fig. 12*D*) but may be related to inhibition of a Na_o^+–Ca_i^{2+} exchange system.

Attempts to pharmacologically disrupt $[Ca^{2+}]_i$ buffering at the level of the Ca^{2+}–Mg^{2+}-ATPase were also without noticeable effect. In erythrocytes calmodulin has been shown to regulate the Ca^{2+}–Mg^{2+}-ATPase (Carafoli, 1984). Thus, it was of interest to superfuse the calmodulin antagonist calmidizolium (10 μM) onto cells in

whole-cell patch-clamp studies. The drug produced a 74% inhibition of the I_{Ca} without affecting $[Ca^{2+}]_i$ buffering rates. In addition when 10 μM-calmidizolium was applied to the cell interior via the patch pipette it produced neither a change in I_{Ca} nor $[Ca^{2+}]_i$ buffering ($n = 5$). We also tried the non-specific ATPase inhibitor sodium orthovanadate which was without effect when applied externally (1 mM; $n = 5$) or in the patch pipette (10 μM; $n = 10$). This finding is also in agreement with Nohmi & Kuba (1984), suggesting that the mechanism of $[Ca^{2+}]_i$ buffering in the cell bodies of intact peripheral neurones may be somewhat different from that found in squid axon and rat brain synaptosomes.

DISCUSSION

We have studied the $[Ca^{2+}]_i$ buffering properties of DRG neurones grown in primary culture by employing the whole-cell patch-clamp technique in combination with Fura-2 ratio microfluorimetry, enabling us to record I_{Ca} and $[Ca^{2+}]_i$ simultaneously. Under our conditions depolarization of DRG neurones for 320 ms or less activated an I_{Ca} which produced a $[Ca^{2+}]_i$ transient that correlated with the rate of Ca^{2+} influx. Thus, for small Ca^{2+} loads the $[Ca^{2+}]_i$ was proportional to the amount of Ca^{2+} flowing into the cell via voltage-sensitive Ca^{2+} channels (Fig. 2*A*). The $[Ca^{2+}]_i$ was considerably lower than the predicted $[Ca^{2+}]_i$ calculated from the amount of charge flowing into the cell via Ca^{2+} channels. Exact calculation of expected values is problematic because of the difficulty in determining the cell volume. This problem has been discussed previously (Pusch & Neher, 1988). However, we have calculated the cell volume (v) from both the measured capacitance and the observed radius (r). The cell was assumed to be spherical, had an experimentally measured capacitance of 51 pF and we assumed the capacitance of biological membranes to be 10^6 pF/cm^2. Thus

$$r = \sqrt{\frac{51 \text{ pF}}{4\pi(10^6 \text{ pF/cm}^2)}} = 20 \ \mu\text{m}.$$

This radius was in good agreement with the radius we observed of 18 μm supporting the assumption that this cell was approximately spherical. The cell volume was calculated using an average radius of 19 μm.

$$\begin{aligned} v &= 4/3\pi r^3 \\ &= 4/3\pi(19 \times 10^{-6} \text{ m})^3 \\ &= 2{\cdot}9 \times 10^{-14} \text{ m}^3 = 2{\cdot}9 \times 10^{-11} \text{ l}. \end{aligned}$$

This cell displayed an integrated I_{Ca} *versus* $[Ca^{2+}]_i$ curve which reached an asymptote at 300 nM with Ca^{2+} influx values as high as 1000 pC. Thus if the cell did not buffer the Ca^{2+} load the $[Ca^{2+}]_i$ would be expected to rise to:

$$\begin{aligned} [Ca^{2+}]_i &= \text{charge}/(2Fv) \\ &= \frac{10^{-9} \text{ C}}{2(9{\cdot}6 \times 10^4 \text{ C/mol})\,(2{\cdot}9 \times 10^{-11} \text{ l})} \\ &= 1{\cdot}8 \times 10^{-4} \text{ M}. \end{aligned}$$

Thus, only 1/600th of the Ca^{2+} load was seen as free Ca^{2+} at the peak of the $[Ca^{2+}]_i$ transient. A smaller Ca^{2+} load of 100 pC was also applied to this cell resulting in a peak $[Ca^{2+}]_i$ of 100 nM, some 180 times smaller than the calculated value. These values are in reasonable agreement with calculations of McBurney & Neering (1985) which predicted that less than 1% of a Ca^{2+} load remained free in the cytosol at the peak of a $[Ca^{2+}]_i$ transient.

In spite of the efficient buffering of Ca^{2+} by the cell, the $[Ca^{2+}]_i$ remained elevated long after the Ca^{2+} influx had ceased. This observation is in good agreement with similar findings in neurones from the rat spinal cord and invertebrates (Mayer *et al.* 1987; Ross *et al.* 1987; Ahmed & Connor, 1988). In DRG neurones we found that buffering of this long-lasting $[Ca^{2+}]_i$ transient could be best described by a single-exponential equation. This is in agreement with studies on invertebrate neurones (Ahmed & Connor, 1988) and in contrast to studies on rat spinal cord (Mayer, 1987). This finding suggests that a single buffering process is dominant in DRG cells under our experimental conditions.

A linear relationship between I_{Ca} and the resulting $[Ca^{2+}]_i$ transient was maintained for a series of modest Ca^{2+} loads applied to a cell by stepping to different test potentials (Fig. 3). The resulting current–voltage curve was similar to that described for chick DRG neurones consistent with the presence of three types of Ca^{2+} channels in the rat DRG neurones as well (Nowycky *et al.* 1985; Fox *et al.* 1987). Even activating the T-type ('low-threshold') current produced a detectable increase in $[Ca^{2+}]_i$ indicating that small depolarizations from hyperpolarized membrane potentials will produce small but significant increases in the $[Ca^{2+}]_i$. The $[Ca^{2+}]_i$ *versus* voltage curve closely paralleled the current–voltage curve indicating that the $[Ca^{2+}]_i$ transient resulted primarily from the influx of Ca^{2+} via voltage-activated Ca^{2+} channels. Thus, voltage-dependent or Ca^{2+}-induced release of Ca^{2+} from intracellular stores did not contribute significantly to the $[Ca^{2+}]_i$ transient in these experiments. This finding is in contrast to the large amplification of the depolarization-induced $[Ca^{2+}]_i$ transient seen in cardiac muscle in which Ca^{2+} influx accounts for only about 10% of the $[Ca^{2+}]_i$ transient. The remaining 90% of the transient is released from a ryanodine-sensitive Ca^{2+} store (Callewaert *et al.* 1988). We have previously reported the presence of ryanodine-sensitive Ca^{2+} stores in rat sympathetic neurones which produce a small amplification of depolarization-induced $[Ca^{2+}]_i$ transients (Thayer *et al.* 1988*a*), and this may be more pronounced in other species (Lipscombe *et al.* 1988). We have also previously shown that similar ryanodine-sensitive stores are present in rat DRG neurones (Thayer *et al.* 1988*b*). However, they are considerably smaller than those found in sympathetic neurones and we were not able to demonstrate a significant Ca^{2+}-induced release of Ca^{2+} in these cells (data not shown). In our experiments spatial resolution has been compromised in order to obtain good time resolution and this may preclude observing Ca^{2+}-induced Ca^{2+} release in localized portions of the cell. Digital imaging techniques may reveal more subtle and localized amplification effects.

When the cell was presented with Ca^{2+} loads of different magnitude the relationship between the integrated I_{Ca} and the peak of the $[Ca^{2+}]_i$ transient reached an asymptote. This observation is consistent with the hypothesis that $[Ca^{2+}]_i$ buffering mechanisms are more efficient when $[Ca^{2+}]_i$ is elevated above some threshold level.

Ahmed & Connor (1988) came to a similar conclusion in their studies on molluscan neurones when they observed that the Ca^{2+} buffering capacity increased with larger Ca^{2+} loads. They also found that Ca^{2+} loads were buffered at different rates depending on how the Ca^{2+} load was applied to the cell. We have not presented an extensive kinetic analysis of the recovery process here. However, limited studies did indicate that the process was described by a single exponential and that the time constant decreased with increased Ca^{2+} loads (Fig. 2*B*). We found that the integral of the I_{Ca} was related to the peak of the $[Ca^{2+}]_i$ transient in an asymptotic manner regardless of whether the Ca^{2+} load was varied by changing the test pulse potential or duration. In the experiments described here the increase in Ca^{2+} buffering efficiency for large loads appears to occur because the mitochondria sequester more Ca^{2+} as the $[Ca^{2+}]_i$ approaches the mitochondrial Ca^{2+} uptake set-point.

The importance of the mitochondrial Ca^{2+} uptake system to $[Ca^{2+}]_i$ buffering in DRG neurones was demonstrated most dramatically in the superfusion experiments described in Figs 12 and 13. It is clear that removing the mitochondrial $[Ca^{2+}]_i$ buffering component by application of the uncoupling agent CCCP considerably shortened the duration of the $[Ca^{2+}]_i$ transient elicited by membrane depolarization (Fig. 12). Inhibition of this $[Ca^{2+}]_i$ buffering mechanism allowed $[Ca^{2+}]_i$ levels to rise significantly above control values while recovery was actually somewhat faster. The observations that little Ca^{2+} was released from the mitochondria when the uncoupler was added under basal conditions and the elevated peak of the $[Ca^{2+}]_i$ transient upon subsequent depolarization support the hypothesis that the mitochondria sequester Ca^{2+} only at relatively elevated levels and that their large capacity serves as a temporary sink for Ca^{2+} during potentially toxic Ca^{2+} loads. As shown in Fig. 12*C* shortly after activation of Ca^{2+} channels the mitochondria contain significant quantities of Ca^{2+}. It is of interest to note that in this protocol the $[Ca^{2+}]_i$ was buffered back to basal levels over the same time span in control and after CCCP treatment, suggesting that the mitochondria are serving as a temporary sink for Ca^{2+} and that the process which actually removes the Ca^{2+} from the cytoplasm is maximally activated during both control and uncoupler-treated $[Ca^{2+}]_i$ transients. Nicholls (1978, 1985) has proposed a role for the mitochondria in protecting the cell from Ca^{2+} overload and has suggested that mitochondria sequester Ca^{2+} when the $[Ca^{2+}]_i$ is elevated above a set-point and release Ca^{2+} when the $[Ca^{2+}]_i$ is below the set-point. We propose that the plateau phase of the 50 mM-K^+-induced $[Ca^{2+}]_i$ transient is the mitochondrial set-point in DRG neurones. Calcium efflux from mitochondria occurs via a Na_o^+–Ca_i^{2+} exchange mechanism. Thus reducing the cytosolic $[Na^+]$ will decrease Ca^{2+} efflux from the mitochondria resulting in an increase in the affinity of the mitochondrial Ca^{2+} uptake process. As predicted, removing extracellular Na^+, a procedure that presumably leads to reduced $[Na^+]_i$, reduced the height of the plateau phase of the $[Ca^{2+}]_i$ transient (Fig. 12*C*) consistent with the plateau height being determined by the mitochondrial set-point for Ca^{2+} uptake. Indeed treatment with CCCP confirmed that the mitochondria contained large amounts of Ca^{2+} during the plateau phase in Na^+-free media. If the mitochondria play a role in protecting the cell from Ca^{2+} overload then the reduced mitochondrial affinity for Ca^{2+} when intracellular Na^+ is elevated would be expected to compromise Ca^{2+} buffering which could be potentially toxic. For example excitatory amino acid-induced neurotoxicity,

in which Ca^{2+} overload is thought to mediate cell death (Choi, 1987), may be particularly effective because of the combined Ca^{2+} and Na^+ load applied to the cell through activation of mono- and divalent permeable cation channels (Murphy, Thayer & Miller, 1987).

Experiments utilizing Ruthenium Red also supported the role of mitochondria in DRG neurone Ca^{2+} buffering. Including Ruthenium Red in the patch pipette removed the high-capacity buffering component which is responsible for the asymptotic shape of the Ca^{2+} influx *versus* $[Ca^{2+}]_i$ curve observed when large Ca^{2+} loads were applied to the cell. This finding is consistent with the studies of Baker & Umbach (1987) on squid axoplasm. They found that Ruthenium Red left basal $[Ca^{2+}]_i$ unchanged but greatly reduced the capacity to buffer additional Ca^{2+} loads. Ruthenium Red has a number of different effects. For example it has also been observed to block Ca^{2+} release from intracellular stores. However, blockade of mitochondrial Ca^{2+} uptake appears to be the action that is most consistent with our observations. A technical point regarding the interpretation of the Ruthenium Red experiments should be considered. Namely, because Ruthenium Red was added directly to the patch pipette we could not determine at what level of Ca^{2+} influx that particular cell would have approached an asymptote. However, as four out of four cells displayed a linear Ca^{2+} influx *versus* $[Ca^{2+}]_i$ relationship in the presence of Ruthenium Red (Fig. 14) compared to ten out of forty in the absence of drug, these data together with the superfusion experiments with CCCP (Fig. 12) provide compelling evidence demonstrating mitochondrial Ca^{2+} buffering in these cells.

It is interesting to note that the plateau $[Ca^{2+}]_i$ observed in the superfusion experiments as well as the $[Ca^{2+}]_i$ asymptote observed in voltage-clamp studies occur at $[Ca^{2+}]_i < 10^{-6}$ M. This implies that significant Ca^{2+} uptake into the mitochondria occurs in the physiological range of $[Ca^{2+}]_i$. Most physiological stimuli that regulate $[Ca^{2+}]_i$ either by promoting Ca^{2+} influx or its mobilization from intracellular stores increase $[Ca^{2+}]_i$ to within this range and therefore allow Ca^{2+} to be taken up into the inner mitochondrial matrix. Thus physiological stimuli may influence the activity of several key Ca^{2+}-dependent dehydrogenases. This may be an important mechanism for coupling cellular activity and cellular energy requirements (McCormack & Denton, 1988). Consequently mitochondrial Ca^{2+} uptake may serve a physiological role in addition to protecting cells against the toxic effects of Ca^{2+} overloading.

The mitochondria only temporarily remove Ca^{2+} from the cytoplasm thus acting to damp large increases in $[Ca^{2+}]_i$. It is clear that these organelles do not contain significant amounts of Ca^{2+} under basal conditions (Fig. 12*B*). Thus, some other pump or sequestration mechanism must ultimately be responsible for removing Ca^{2+} from the cytosol. In contrast to studies in squid giant axon (Allen & Baker, 1986) and rat brain synaptosomes (Sanchez-Armass & Blaustein, 1987) but in agreement with studies on frog sympathetic neurone cell bodies (Nohmi & Kuba, 1984), *Aplysia* bag cells (Levy & Tillotson, 1988) and rat DRG neurones (Benham *et al.* 1989) we were not able to demonstrate a significant Na_o^+-dependent Ca_i^{2+} efflux from the cell bodies of rat DRG neurones. In previous studies on central neurones we have shown only a very small transient effect on $[Ca^{2+}]_i$ when replacing extracellular Na^+ with $choline^+$ (Thayer, Murphy & Miller, 1986), similar to the small changes in basal $[Ca^{2+}]_i$ observed here (Figs 12*D* and 15*A*). A plausible explanation for this

discrepancy may be that the Na_o^+–Ca_i^{2+} exchanger plays a more significant role in buffering $[Ca^{2+}]_i$ in the processes and nerve terminals than in the soma. Thus the marked differences in the rate of buffering $[Ca^{2+}]_i$ in DRG cell bodies compared to DRG processes could be accounted for by a differential distribution of the Na_o^+–Ca_i^{2+} exchanger. Consistent with this idea is the larger surface-to-volume ratio of the process relative to the soma. This explanation might also account for the lack of a $[Ca^{2+}]_i$ plateau as well as the smaller peak $[Ca^{2+}]_i$ values in the DRG process. If a Na_o^+–Ca_i^{2+} exchange system were competing with the mitochondria for Ca^{2+} a reduced Ca^{2+} load would accumulate in the mitochondria, thus shortening the plateau.

The apparent discrepancy between the patch-clamp experiments in which removal of extracellular Na^+ produced only minor changes in the basal $[Ca^{2+}]_i$ (Fig. 15) and the dramatic change in the height of the slowly buffered $[Ca^{2+}]_i$ tail seen in the superfusion experiments (Fig. 12*D* and *E*) may be resolved by noting that the patch pipette would be expected to continuously buffer the $[Na^+]_i$. Thus, attempts to alter the $[Na^+]_i$ in the patch-clamp experiments are hindered by the exchange of Na^+ between the cytoplasm and the pipette. The exchange of Ca^{2+} between the cytoplasm and the pipette is also of concern. However, the slow exchange between the pipette and cytoplasm, which occurs in the order of minutes, would be expected to have relatively minor effects on the $[Ca^{2+}]_i$ transients elicited by depolarizing test pulses which last from milliseconds to seconds (Cannell, Berlin & Lederer, 1987).

Because the relationship between the I_{Ca} and the peak $[Ca^{2+}]_i$ becomes asymptotic at large Ca^{2+} loads we would predict that inhibition of Ca^{2+} channels may have relatively minor effects on neurones in which $[Ca^{2+}]_i$ is elevated due to high-frequency or long-duration bursts of action potentials. Our results demonstrating that the relationship between the number of action potentials fired in a high-frequency burst and the resulting increase in $[Ca^{2+}]_i$ approaches an asymptote suggests that modulation of $[Ca^{2+}]_i$ by inhibition of Ca^{2+} channels will be more effective in cells firing at lower frequencies. Indeed many inhibitory neurotransmitters including NPY and opioids, which act presynaptically to inhibit neurotransmitter release, are clearly less effective at elevated firing rates (Budai & Duckles, 1988; Grundemar, Widmark, Waldeck & Hakanson, 1988). Furthermore, Jia & Nelson (1986) have hypothesized that the observed decrement in I_{Ca} and reduced synaptic transmitter output from DRG neurones that results from rapid repetitive stimulation is due to an inability to maintain a low $[Ca^{2+}]_i$. Clearly our results support their conclusion in that we have observed a very slow recovery of the $[Ca^{2+}]_i$ transient to basal levels after application of large Ca^{2+} loads such as those resulting from high-frequency stimulation (Fig. 11).

In summary, therefore, we have shown that bursts of increasing numbers of action potentials or increased duration voltage steps produce increases in $[Ca^{2+}]_i$ that approach an asymptote. This asymptote is the result of a high-capacity mitochondrial Ca^{2+} uptake system and has important implications for the effects of neuromodulators on $[Ca^{2+}]_i$ as well as for the protection of neurones from toxic Ca^{2+} overload.

This work was supported by grants DAO2121, DAO2575 and MH40165 from the National Institutes of Health, and in part by Bayer Inc., Miles Laboratories Inc. and Marion Labs (R.J.M.). S.A.T. was a Senior Fellow of the Chicago Heart Association.

REFERENCES

AHMED, Z. & CONNOR, J. A. (1988). Calcium regulation by and buffer capacity of molluscan neurones during calcium transients. *Cell Calcium* **9**, 57–69.

ALLEN, T. J. A. & BAKER, P. F. (1986). Comparison of the effects of potassium and membrane potential on the calcium-dependent sodium efflux in squid axons. *Journal of Physiology* **378**, 53–76.

BAKER, P. F. & DIPOLO, R. (1984). Axonal calcium and magnesium homeostasis. *Current Topics in Membrane Transport* **22**, 195–247.

BAKER, P. F. & UMBACH, J. A. (1987). Calcium buffering in axons and axoplasm of *Loligo*. *Journal of Physiology* **383**, 369–394.

BARCENAS-RUIZ, L., BEUCKELMANN, D. J. & WIER, W. G. (1987). Sodium–calcium exchange in heart: membrane currents and changes in $[Ca^{2+}]_i$. *Science* **238**, 1720–1722.

BENHAM, C. D., EVANS, M. L. & MCBAIN, C. J. (1989). Inhibition of Ca^{2+} ATPase slows recovery from voltage gated Ca^{2+} load in cultured cells from rat dorsal root ganglion. *Journal of Physiology* **415**, 21*P*.

BLAUSTEIN, M. P. (1988). Calcium and synaptic function. In *Handbook of Experimental Pharmacology*, ed. BAKER, P. F., p. 83. Springer-Verlag.

BOYLE, M. B., KLEIN, M., SMITH, S. J. & KANDEL, E. R. (1984). Serotonin increases intracellular Ca^{2+} transients in voltage-clamped sensory neurones of *Aplysia californica*. *Proceedings of the National Academy of Sciences of the USA* **81**, 7642–7646.

BUDAI, D. & DUCKLES, S. P. (1988). Influence of stimulation train length on the opioid-induced inhibition of norepinephrine release in the rabbit ear artery. *Journal of Pharmacology and Experimental Therapeutics* **247**, 839–843.

CALLEWAERT, G., CLEEMANN, L. & MORAD, M. (1988). Epinephrine enhances Ca^{2+} current-regulated Ca^{2+} release and Ca^{2+} reuptake in rat ventricular myocytes. *Proceedings of the National Academy of Sciences of the USA* **85**, 2009–2013.

CANNELL, M. B., BERLIN, J. R. & LEDERER, W. J. (1987). Effect of membrane potential changes on the calcium transient in single rat cardiac muscle cells. *Science* **238**, 1419–1423.

CARAFOLI, E. (1984). Calmodulin-sensitive calcium-pumping ATPase of plasma membranes: isolation, reconstitution, and regulation. *Federation Proceedings* **43**, 3005–3010.

CARAFOLI, E. (1987). Intracellular calcium homeostasis. *Annual Reviews of Biochemistry* **56**, 395–433.

CHOI, D. W. (1987). Ionic dependence of glutamate neurotoxicity. *Journal of Neuroscience* **7**, 369–379.

CONNOR, J. A., KRETZ, R. & SHAPIRO, D. (1986). Calcium levels measured in a presynaptic neurone of *Aplysia* under conditions that modulate transmitter release. *Journal of Physiology* **375**, 625–642.

EWALD, D. A., STERNWEIS, P. C. & MILLER, R. J. (1988). Guanine nucleotide-binding protein G_o-induced coupling of NYP receptors to Ca^{2+} channels in sensory neurones. *Proceedings of the National Academy of Sciences of the USA* **85**, 3633–3637.

FABIATO, A. (1985*a*). Rapid ionic modifications during the aequorin-detected calcium transient in a skinned cardiac Purkinje cell. *Journal of General Physiology* **85**, 189–246.

FABIATO, A. (1985*b*). Time and calcium dependence of activation and inactivation of calcium-induced release of calcium from the sarcoplasmic reticulum of a skinned cardiac Purkinje cell. *Journal of General Physiology* **85**, 247–289.

FABIATO, A. & FABIATO, F. (1979). Calculator programs for computing the composition of the solutions containing multiple metals and ligands used for experiments in skinned muscle cells. *Journal de physiologie* **75**, 463–505.

FOX, A. P., NOWYCKY, M. C. & TSIEN, R. W. (1987). Kinetic and pharmacological properties distinguishing three types of calcium currents in chick sensory neurones. *Journal of Physiology* **394**, 149–172.

GORMAN, A. L. F. & THOMAS, M. V. (1980). Intracellular calcium accumulation during depolarization in a molluscan neurone. *Journal of Physiology* **308**, 259–285.

GRUNDEMAR, L., WIDMARK, E., WALDECK, B. & HAKANSON, R. (1988). NPY: prejunctional inhibition of vagally induced contractions in the guinea pig trachea. *Regulatory Peptides* **23**, 309–313.

GRYNKIEWICZ, G., POENIE, M. & TSIEN, R. Y. (1985). A new generation of calcium indicators with greatly improved fluorescence properties. *Journal of Biological Chemistry* **260**, 3440–3450.

GUNTER, T. E., WINGROVE, D. E., BANERJEE, S. & GUNTER, K. K. (1988). Mechanisms of mitochondrial calcium transport. *Advanced Experimental Biology* **232**, 1–14.

HAMILL, O. P., MARTY, A., NEHER, E., SAKMANN, B. & SIGWORTH, F. (1981). Improved patch-clamp techniques for high resolution current recording from cells and cell-free membrane patches. *Pflügers Archiv* **391**, 85–100.

JIA, M. & NELSON, P. G. (1986). Calcium currents and transmitter output in cultured spinal cord and dorsal root ganglion neurones. *Journal of Neurophysiology* **56**, 1257–1267.

KOSTYUK, P. G., SHUBA, YA. M. & SAVCHENKO, A. N. (1988). Three types of calcium channels in the membrane of mouse sensory neurones. *Pflügers Archiv* **411**, 661–669.

KUBA, K. (1980). Release of calcium ions linked to the activation of potassium conductance in a caffeine-treated sympathetic neurone. *Journal of Physiology* **298**, 251–269.

LEV-RAM, V. & GRINVALD, A. (1987). Activity-dependent calcium transients in central nervous system myelinated axons revealed by the calcium indicator Fura-2. *Biophysical Journal* **52**, 571–576.

LEVY, S. & TILLOTSON, D. (1988). Effects of Na^{2+} and Ca^{2+} gradients on intracellular free Ca^{2+} voltage-clamped *Aplysia* neurones. *Brain Research* **474**, 333–342.

LIPSCOMBE, D., MADISON, D. V., POENIE, M., REUTER, H., TSIEN, R. W. & TSIEN, R. Y. (1988). Imaging of cytosolic Ca^{2+} transients arising from Ca^{2+} stores and Ca^{2+} channels in sympathetic neurones. *Neuron* **1**, 355–365.

MCBURNEY, R. N. & NEERING, V. (1985). The measurement of changes in intracellular free calcium during action potentials in mammalian neurones. *Journal of Neuroscience Methods* **13**, 65–76.

MCCORMACK, J. G. & DENTON, R. M. (1988). The regulation of mitochondrial function in mammalian cells by Ca^{2+} ions. *Biochemical Society Transactions* **16**, 523–527.

MALGAROLI, A., MILANI, D., MELDOLESI, J. & POZZAN, T. (1987). Fura-2 measurement of cytosolic free Ca^{2+} in monolayers and suspensions of various types of animal cells. *Journal of Cell Biology* **105**, 2145–2155.

MAYER, M. L., MACDERMOTT, A. B., WESTBROOK, G. L., SMITH, S. J. & BARKER, J. L. (1987). Agonist- and voltage-gated calcium entry in cultured mouse spinal cord neurones under voltage clamp measured using arsenazo III. *Journal of Neuroscience* **7**, 3230–3244.

MAYER, M. L. & WESTBROOK, G. L. (1987). The physiology of excitatory amino acids in the vertebrate central nervous system. *Progress in Neurobiology* **28**, 197–276.

MOORE, C. L. (1971). Specific inhibition of mitochondrial Ca^{++} transport by ruthenium red. *Biochemical and Biophysical Research Communications* **42**, 298–305.

MURPHY, S. N., THAYER, S. A. & MILLER, R. J. (1987). The effects of excitatory amino acids on intracellular calcium in single mouse striatal neurones in vitro. *Journal of Neuroscience* **7**, 4145–4158.

NICHOLLS, D. G. (1978). The regulation of extramitochondrial free calcium ion concentration by rat liver mitochondria. *Biochemical Journal* **176**, 463–474.

NICHOLLS, D. G. (1985). A role for the mitochondrion in the protection of cells against calcium overload? *Progress in Brain Research* **63**, 97–106.

NOHMI, M. & KUBA, K. (1984). Effects of Na^{+} gradient on the intracellular Ca^{2+} oscillation in the sympathetic ganglion cell: Na–Ca exchange in the neurone cell soma? *Brain Research* **324**, 171–174.

NOWYCKY, M. C., FOX, A. P. & TSIEN, R. W. (1985). Three types of neuronal calcium channel with different calcium agonist sensitivity. *Nature* **316**, 440–443.

PUSCH, M. & NEHER, E. (1988). Rates of diffusional exchange between small cells and a measuring patch pipette. *Pflügers Archiv* **411**, 204–211.

ROSS, W. N., ARECHIGA, V. & NICHOLLS, J. G. (1987). Optical recording of calcium and voltage transients following impulses in cell bodies and processes of identified leech neurones in culture. *Journal of Neuroscience* **7**, 3877–3887.

ROSS, W. N. & GRAUBARD, K. (1989). Spatially and temporally resolved calcium concentration changes in oscillating neurones of crab stomatogastric ganglion. *Proceedings of the National Academy of Sciences of the USA* **86**, 1679–1683.

SANCHEZ-ARMASS, S. & BLAUSTEIN, M. P. (1987). Role of sodium–calcium exchange in regulation of intracellular calcium in nerve terminals. *American Journal of Physiology* **252**, C595–603.

STREB, H. P., IRVINE, R. F., BERRIDGE, M. J. & SCHULZ, I. (1983). Release of Ca^{2+} from a nonmitochondrial intracellular store in pancreatic acinar cells by inositol-1,4,5-trisphosphate. *Nature* **306**, 67–69.

TANK, D. W., SUGIMORI, M., CONNOR, J. A. & LLINAS, R. R. (1988). Spatially resolved calcium dynamics of mammalian Purkinje cells in cerebellar slice. *Science* **242**, 773–777.

THAYER, S. A., HIRNING, L. D. & MILLER, R. J. (1987). Distribution of multiple types of Ca^{2+} channels in rat sympathetic neurons *in vitro*. *Molecular Pharmacology* **32**, 579–586.

THAYER, S. A., HIRNING, L. D. & MILLER, R. J. (1988*a*). The role of caffeine sensitive calcium stores in the regulation of free intracellular calcium in rat sympathetic neurones *in vitro*. *Molecular Pharmacology* **34**, 664–673.

THAYER, S. A. & MILLER, R. J. (1988). Relationship between calcium currents and intracellular calcium concentration in sensory neurons. *Society for Neuroscience Abstracts* **14**, 900.

THAYER, S. A., MURPHY, S. N. & MILLER, R. J. (1986). Widespread distribution of dihydropyridine-sensitive calcium channels in the central nervous system. *Molecular Pharmacology* **30**, 505–509.

THAYER, S. A., PERNEY, T. M. & MILLER, R. J. (1988*b*). Regulation of calcium homeostasis in sensory neurones by bradykinin. *Journal of Neuroscience* **8**, 4089–4097.

THAYER, S. A., STUREK, M. & MILLER, R. J. (1988*c*). Measurement of neuronal Ca^{2+} transients using simultaneous microfluorimetry and electrophysiology. *Pflügers Archiv* **412**, 216–223.

TSIEN, R. W. (1983). Calcium channels in excitable cell membranes. *Annual Review of Physiology* **45**, 341–358.

ZUCKER, R. S. (1981). Tetraethylammonium contains an impurity which alkalizes cytoplasm and reduces calcium buffering in neurones. *Brain Research* **208**, 473–478.